remote sensing

MDPI

Article

Evaluation of Bias Correction Methods for GOSAT SWIR XH_2O Using TCCON data

Tran Thi Ngoc Trieu [1,*], Isamu Morino [1], Hirofumi Ohyama [1], Osamu Uchino [1], Ralf Sussmann [2], Thorsten Warneke [3], Christof Petri [3], Rigel Kivi [4], Frank Hase [5], David F. Pollard [6], Nicholas M. Deutscher [7], Voltaire A. Velazco [7], Laura T. Iraci [8], James R. Podolske [8] and Manvendra K. Dubey [9]

1 Satellite Observation Center, National Institute for Environmental Studies (NIES), 16-2 Onogawa, Tsukuba 305-8506, Japan; morino@nies.go.jp (I.M.); oyama.hirofumi@nies.go.jp (H.O.); uchino.osamu@nies.go.jp (O.U.)
2 IMK-IFU, Karlsruhe Institute of Technology, 82467 Garmisch-Partenkirchen, Germany; ralf.sussmann@kit.edu
3 Institute of Environmental Physics, University of Bremen, Otto-Hahn- Allee 1, 28359 Bremen, Germany; warneke@iup.physik.uni-bremen.de (T.W.); christof.petri@iup.physik.uni-bremen.de (C.P.)
4 Space and Earth Observation Centre, Finnish Meteorological Institute, Tähteläntie 62, 99600 Sodankylä, Finland; rigel.kivi@fmi.fi
5 IMK-ASF, Karlsruhe Institute of Technology, Hermann-von-Helmholtz-Platz 1, 76344 Leopoldshafen, Germany; frank.hase@kit.edu
6 National Institute of Water and Atmospheric Research Ltd. (NIWA), State Highway 85, Lauder, Omakau, Central Otago 9377, New Zealand; Dave.Pollard@niwa.co.nz
7 Centre for Atmospheric Chemistry, Faculty of Science, Medicine and Health, University of Wollongong, Northfields Ave, Wollongong NSW 2522, Australia; ndeutsch@uow.edu.au (N.M.D.); voltaire@uow.edu.au (V.A.V.)
8 Atmospheric Science Branch, NASA Ames Research Center, Mail Stop 245-5, Moffett Field, CA 94035, USA; Laura.T.Iraci@nasa.gov (L.T.I.); James.R.Podolske@nasa.gov (J.R.P.)
9 Los Alamos National Laboratory, Los Alamos, NM 87545, USA; dubey@lanl.gov
* Correspondence: ttntrieu@gmail.com; Tel.: +81-29-850-2798

Received: 19 December 2018; Accepted: 29 January 2019; Published: 1 February 2019

Abstract: This study evaluated three bias correction methods of systematic biases in column-averaged dry-air mole fraction of water vapor (XH_2O) data retrieved from Greenhouse Gases Observing Satellite (GOSAT) Short-Wavelength Infrared (SWIR) observations compared with ground-based data from the Total Carbon Column Observing Network (TCCON). They included an empirically multilinear regression method, altitude bias correction method, and combination of altitude and empirical correction for three cases defined by the temporal and spatial collocation around TCCON site. The results showed that large altitude differences between GOSAT observation points and TCCON instruments are the main cause of bias, and the altitude bias correction method is the most effective bias correction method. The lowest biases result from GOSAT SWIR XH_2O data within a $0.5^\circ \times 0.5^\circ$ latitude $\times$ longitude box centered at each TCCON site matched with TCCON XH_2O data averaged over $\pm$15 min of the GOSAT overpass time. Considering land data, the global bias changed from $-1.3 \pm 9.3\%$ to $-2.2 \pm 8.5\%$, and station bias from $-2.3 \pm 9.0\%$ to $-1.7 \pm 8.4\%$. In mixed land and ocean data, global bias and station bias changed from $-0.3 \pm 7.6\%$ and $-1.9 \pm 7.1\%$ to $-0.8 \pm 7.2\%$ and $-2.3 \pm 6.8\%$, respectively, after bias correction. The results also confirmed that the fine spatial and temporal collocation criteria are necessary in bias correction methods.

Keywords: GOSAT SWIR XH_2O; systematic biases; bias correction; TCCON XH_2O; altitude bias correction

1. Introduction

Atmospheric water vapor is extremely important in both meteorological and climatological studies [1,2] and its distribution is characterized by very high temporal and spatial variability. Knowledge of its distribution and how it will be affected by the changing climate is critical to our understanding of the Earth's climate system. Satellite-borne instruments have an advantage over ground-based instruments because they have global coverage. Various satellite-borne sensors use different measurement techniques and observation geometries (e.g., nadir sounding and limb sounding) for measurements in different spectral domains and at different altitude ranges [3]. Accurate measurements of water vapor concentration are essential to understand its effect on weather and climate [4]. Before using satellite water vapor data, intrinsic biases in the data must be assessed and removed [5] by comparing the satellite data with independently obtained ground-based data. Such comparisons must address spatial and temporal inconsistencies between the two types of data, which account for most of the scatters and biases [6–8]. Although many studies have investigated bias of satellite data [9–11], few studies have attempted bias correction of satellite water vapor [7].

The Greenhouse Gases Observing Satellite (GOSAT) is a Japanese satellite dedicated to measuring concentrations of atmospheric greenhouse gases such as CO_2, CH_4, and H_2O. GOSAT was launched in January 2009 in a sun-synchronous orbit: it has a 98° inclination at an altitude of 666 km and crosses the equator at 12:48 local time [12]. Column-averaged dry-air mole fractions of H_2O (XH_2O) are retrieved from the Short-Wavelength InfraRed (SWIR) spectra of the thermal and near-infrared sensor for carbon observation-Fourier transform spectrometer (TANSO-FTS) on GOSAT.

The Total Carbon Column Observing Network (TCCON) is a worldwide network of ground-based FTSs whose main purpose is to provide reliable, long-term time series of column-averaged abundances of greenhouse gases and other atmospheric constituents for carbon cycle studies and for validating satellite measurements [13].

Bias in water vapor measurements has recently been the focus of several multi-instrument comparison studies. Some studies compared integrated water vapor (IWV) measurements in locations spanning the Arctic to the tropics among instruments: Global Navigation Satellite Systems (GNSS), Atmospheric Infrared Sounder (AIRS), Moderate Resolution Imaging Spectrometer (MODIS), Scanning Imaging Absorption Spectrometer for Atmospheric CHartographY (SCIAMACHY), radiosondes, Global Positioning System (GPS), GOME, ground-based FTIR, ground-based microwave radiometer, and satellite-based Advanced Microwave Sounding Unit (AMSU-B), Vaisala RS-80 A-HUMICAP radiosondes, and very-long-baseline interferometry [14–17]. In addition, there were studies looking at the biases in multisite intercomparisons of water vapor observations [18–24]. Biases in XCH_4 and XCO_2 from GOSAT retrievals have also been studied recently [25–30], but investigations of bias in GOSAT XH_2O data retrieved by the National Institute for Environmental Studies (NIES) full-physics algorithm are scarce. Dupuy et al. [31] performed statistical comparisons and estimated bias without bias correction, and Ohyama et al. [7] assessed measurement precision by comparing two XH_2O data products retrieved independently from thermal infrared (TIR) and SWIR spectral radiances measured by the TANSO-FTS onboard GOSAT with TCCON XH_2O data. Trent et al. [32] used the University of Leicester Full-Physics GOSAT SWIR XH_2O retrieval for estimation of a new water vapor dataset in the planetary boundary layer with a low bias compared with global radiosonde data. All these studies used only land data, however.

In this study, we used both land data and mixed ocean and land data from the NIES Full-Physics GOSAT SWIR XH_2O retrieval to evaluate three bias correction methods—empirically derived bias correction, altitude bias correction, and altitude bias correction—followed by empirically derived bias correction. The paper is structured as follows. Section 2 briefly presents the datasets used and describes the analysis procedures in detail. In Section 3, we present our bias correction results. In Section 4, we discuss these results in detail. Our conclusions are presented in Section 5.

2. Data and Methods

2.1. Data

We used GOSAT SWIR XH_2O data version 02.72 (the latest version) for the period from April 2009 to December 2017 [33]. GOSAT data are divided into six categories: sounding over ocean (ocean data) acquired in gain H amplification mode, ocean data (gain M), sounding over land (land data) (gain H), land data (gain M), sounding over mixed land and ocean (mixed data) (gain H), and mixed data (gain M). The land fraction of land data is 100% whereas in mixed data (i.e., observations made over land and ocean at the vicinity of coastlines, lakes), it is >60% but < 100%. However, because insufficient ocean data and gain-M data were available, we only analyzed land data and mixed data acquired with gain-H amplification mode. Although described in Suto et al. [34], band 1 (0.76 μm), band 2 (1.6 μm), and band 3 (2.0 μm) of SWIR could be measured with three gains including high (H), medium (M), and low (L), GOSAT uses gain-H for most soundings over land and ocean and gain-M for soundings over bright surfaces in the SWIR as deserts and semi-arid regions (e.g., Sahara, Nevada, and central Australia) [35].

For reference values, we used version GGG2014 TCCON data [36] from 18 ground-based TCCON sites: Sodankylä [37], Bialystok [38], Bremen [39], Karlsruhe [40], Orléans [41], Garmisch [42], Park Falls [43], Rikubetsu [44], Four Corners [45], Lamont [46], Tsukuba [47], Dryden [48], JPL [49], Caltech [50], Saga [51], Darwin [52], Wollongong [53], and Lauder [54,55] (Figure 1). These data include updates through October 2017.

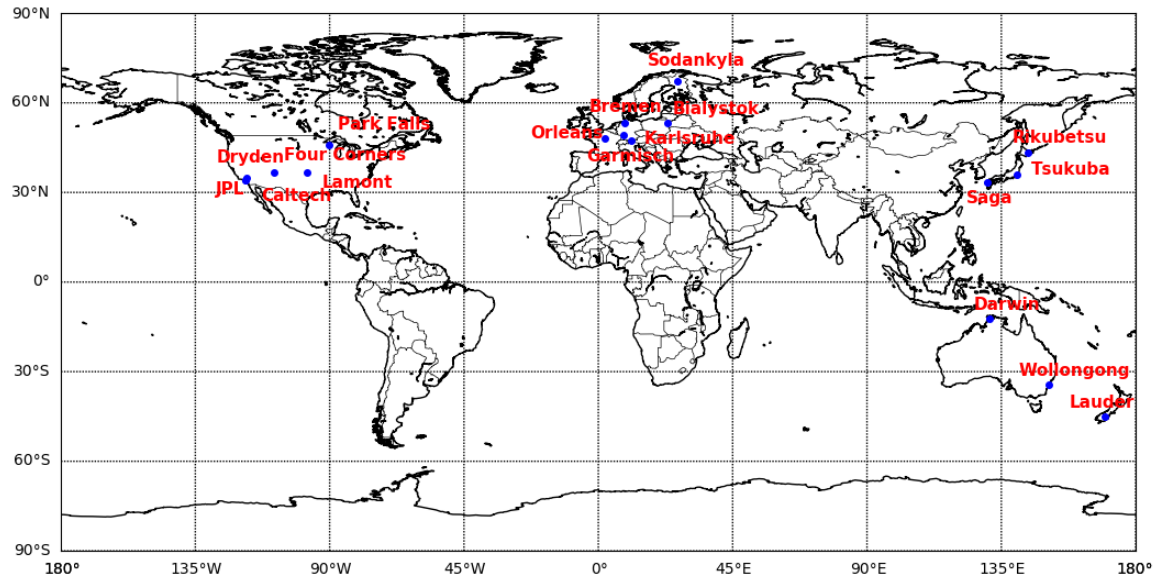

Figure 1. Global map of the ground-based Total Carbon Column Observing Network (TCCON) sites used for correction and validation of Greenhouse Gases Observing Satellite (GOSAT) data.

Systematic bias in the GOSAT SWIR XH_2O retrievals is caused by many factors. The choice of the forward model itself leads to systematic bias; the ill-posed retrieval problem might also contribute. There are artificial correlations between retrieved XH_2O values and simultaneously derived auxiliary parameters such as optical depth, elevation of the GOSAT observation point, and air mass and surface pressure retrieval errors. The systematic bias can be calculated by a simple empirical multiple linear regression analysis of the correlated variabilities of the XH_2O retrieval and these retrieved auxiliary parameters. In addition, retrieval results obtained from two different instruments with different viewing geometries differ because of differences in their retrieval algorithms, a priori profiles, and averaging kernels. GOSAT SWIR XH_2O data, together with XCO_2 and XCH_4 data, are retrieved by the NIES operational retrieval algorithm [29,31]. It takes four steps to retrieve these data:

prescreening filter to reject cloud contaminated measurements using the TANSO-CAI cloud-detection algorithm; preprocessing to remove further cloudy observations by a CAI "spatial coherence" and a "2 μm-scattering" tests; applying the forward model to fit four spectral regions from Bands 1, 2 and 3 of TANSO-FTS including the oxygen "O_2-A" subband (12,950–13,200 cm $^{-1}$), the "weak CO_2" subband (6180–6380 cm^{-1}), the CH_4 subband (5900–6150 cm^{-1}), and the "strong CO2" subband (4800–4900 cm^{-1}) at the same time; and last screening step for quality check. XH_2O, XCO_2, and XCH_4 data are converted from H_2O, CO_2, and CH_4 vertical column densities, respectively, which are obtained by integrating their partial columns. These H_2O, CO_2, and CH_4 partial columns are derived over 15 vertical layers, together with aerosol and surface pressure parameters. The surface albedo in land soundings and the surface wind speed in ocean soundings are also retrieved.

TCCON XH_2O data are retrieved by the GFIT algorithm [13] scaled to an a priori profile from the National Centers for Environmental Prediction reanalysis data [56] to produce a best-fit synthetic spectrum for the measured spectrum. As described in Ohyama et al. [7], the effect of the difference in the a priori profile between the TCCON instruments and GOSAT on the GOSAT SWIR XH_2O bias was only 0.21%, and the effects of column-averaging kernel differences were very small, therefore these were not taken into account in our analysis. Dupuy et al. [31] reported a bias of −3.1% (±9.5–17.7%) in the GOSAT SWIR XH_2O measurements (ver. 02.21) against the TCCON data that they attributed to the altitude difference between GOSAT observation points and TCCON instruments.

2.2. Methods

We selected three different sets of geophysical collocation criteria because of the very high spatial and temporal variabilities of atmospheric water vapor [20], referred to as cases 0–2, to use in our analysis: case 0, GOSAT SWIR XH_2O data retrieved in ±0.5° latitude/longitude boxes centered at each TCCON site were collocated with the mean values of TCCON data measured within ±15 min of the corresponding GOSAT overpass time; case 1, GOSAT SWIR XH_2O data retrieved in ±1° latitude/longitude boxes centered at each TCCON site were collocated with the mean values of TCCON data measured within ± 30 min of the corresponding GOSAT overpass time; and case 2, GOSAT SWIR XH_2O data retrieved in ±2° latitude/longitude boxes centered at each TCCON site were collocated with the mean values of TCCON data measured within ±30 min of the corresponding GOSAT overpass time. The selection of collocation criteria is an important part of satellite data validation and assessment [57,58]. We applied the three bias correction methods to each collocation case.

2.2.1. Empirically Derived Bias Correction

To correct for the systematic bias in XH_2O retrievals, we applied an empirically derived bias correction method (E) [59] to GOSAT SWIR XH_2O by conducting multilinear regression analyses between the GOSAT biases and simultaneously retrieved auxiliary parameters. The correlation analysis results were used to correct for the systematic bias in the GOSAT data by removing incorrect correlations. We used data from the 18 TCCON sites as reference values in the regression analyses. Regression variables and correlation coefficients were determined separately for land and mixed GOSAT data.

The differences between the original GOSAT XH_2O data and the TCCON XH_2O data were referred to as ΔXH_2O that were determined for all three collocation cases. We selected five retrieved parameters to examine systematic bias in GOSAT SWIR XH_2O land data: surface pressure (P), altitude difference (ΔZ) between the GOSAT observation and TCCON site (TCCON minus GOSAT), albedo in the CO_2 subband 6255 cm $^{-1}$ (Alb_1), albedo in the O_2 subband 13,200 cm^{-1} (Alb_2), and air mass (air mass = $1/\cos\theta_Z + 1/\cos\theta_V$, where θ_Z is the solar zenith angle and θ_V is the satellite-viewing angle). For mixed data, we selected aerosol optical depth at 1.6 μm ($AOD_{1.6}$), temperature shift (T) (a difference from a priori temperature), air mass, Alb_1, and Alb_2. The bias corrections were calculated as follows.

For land data,

$$XH_2O_{corrected} = XH_2O_{retrieved} + C_0 + C_1\left(P - \overline{P}\right) + C_2\left(\Delta Z - \overline{\Delta Z}\right) + C_3\left(Alb_1 - \overline{Alb_1}\right) + C_4\left(Alb_2 - \overline{Alb_2}\right) + C_5\left(airmass - \overline{airmass}\right) \quad (1)$$

and for mixed data,

$$XH_2O_{corrected} = XH_2O_{retrieved} + C_0 + C_1\left(AOD_{1.6} - \overline{AOD_{1.6}}\right) + C_2\left(T - \overline{T}\right) + C_3\left(Alb_1 - \overline{Alb_1}\right) + C_4\left(Alb_2 - \overline{Alb_2}\right) + C_5\left(airmass - \overline{airmass}\right) \quad (2)$$

The overbars denote the averages of all GOSAT data used for the regression analysis. The coefficients of C_0, C_1, C_2, C_3, C_4, and C_5, estimated by multiple linear regression for land data and mixed data, are presented in Table 1a.

2.2.2. Altitude Bias Correction

To correct for bias caused by the altitude differences between TCCON sites and GOSAT observation points, we used the method of Ohyama et al. [7], referred to here as bias correction method (A). We corrected for XH_2O bias caused by the altitude differences by individually adjusting integrated water vapor (C_{IWV}) and dry-air column (C_{Air}) data from GOSAT SWIR to those at the TCCON site elevation. The corrected IWV value (C'_{IWV}) was obtained as follows.

$$C'_{IWV} = C_{IWV}\,(1 + \Gamma \times \Delta h). \quad (3)$$

The corrected total dry-air column value (C'_{Air}) was calculated by the following equation.

$$C'_{Air} = C_{Air}\,\exp(\Delta h / h_s). \quad (4)$$

In these equations, Δh is the altitude difference between the GOSAT observation and the TCCON site (GOSAT minus TCCON); and $h_s = RT_g/Mg$ is the scale height, where R is the molar gas constant, M is the average molecular weight of wet air (28.97 g·mol^{-1}), g is gravitational acceleration, and T_g is atmospheric temperature measured at each TCCON site which was included in the TCCON data. Γ, which is the rate of change in IWV with respect to altitude, was determined for each TCCON site by using radiosonde data from the closest Integrated Global Radiosonde Archive station [60]. For the TCCON sites at Sodankylä, Bialystok, Karlsruhe, Orléans, Garmisch, Park Falls, Four Corners, Lamont, Tsukuba, Saga, JPL, Darwin, Wollongong, and Lauder, we used monthly mean Γ values derived by Ohyama et al. [7] and extended them to December 2017. We derived new Γ values for the sites at Bremen, Rikubetsu, and Dryden, and for the Caltech site, we used Γ derived for the neighboring JPL site. The radiosonde sites and the derived Γ values corresponding to each TCCON site are listed in Tables A1 and A2 in the Appendix A.

Table 1. Regression coefficients and their standard errors for the three colocation cases for the (a) bias-correction method (E) and (b) bias-correction method (A + E). The units of coefficients C_0, C_1, C_2, (C_3, C_4), and C_5 are (ppm), (ppm/hPa), (ppm/m), (ppm/units of albedo), and (ppm/air mass) for GOSAT Short-Wavelength Infrared (SWIR) column-averaged dry-air mole fractions of H_2O (XH_2O) land data and (ppm), (ppm/units of AOD), (ppm/K), (ppm/units of albedo), and (ppm/air mass) for GOSAT SWIR XH_2O mixed data. Case 0, GOSAT retrievals within ±0.5° centered at each TCCON site and TCCON data averaged over ±15 min of the GOSAT overpass time; case 1, within ±1.0° and ±30 min and case 2, within ±2.0° and ±30 min.

	GOSAT SWIR XH_2O (Land)						**GOSAT SWIR XH_2O (Mixed)**					
	Case 0		**Case 1**		**Case 2**		**Case 0**		**Case 1**		**Case 2**	
Coeff.	**Value**	**Std. err.**	**Value**	**Std. err.**	**Value**	**Std. err.**	**Value**	**Std. err.**	**Value**	**Std. err.**	**Value**	**Std. err.**
(a)												
C_0	30.41	3.55	58.28	5.11	51.49	4.93	17.39	5.73	49.94	8.77	38.32	9.07
C_1	−0.25	0.11	−4.10	0.56	−4.5	0.54	209.05	462.51	123.02	624.77	−220.91	639.39
C_2	−0.59	0.02	−0.14	0.06	−0.15	0.06	−27.83	17.01	111.73	25.30	25.77	25.46
C_3	774.07	129.79	1058.38	122.16	717.61	100.52	−60.58	231.38	2442.87	208.43	1531.82	206.31
C_4	149.15	138.78	111.58	160.08	343.22	136.32	286.69	156.48	828.62	208.76	530.42	223.25
C_5	13.055	11.26	22.28	16.05	16.2	15.27	−9.49	25.84	−12.51	33.29	−35.66	33.33
(b)												
C_0	55.18	3.46	77.57	4.57	85.69	36.96	29.03	5.37	46.29	7.65	67.83	8.31
C_1							−336.95	433.44	−138.58	545.05	186.47	585.96
C_2							−1.79	15.94	36.37	22.07	37.79	23.34
C_3	925.44	126.58	1120.06	103.82	1204.99	97.12	317.59	216.84	723.22	181.83	1139.28	189.07
C_4	−213.93	131.84	52.69	143.47	415.29	133.43	89.49	146.64	365.49	182.12	279.05	204.59
C_5	−16.64	10.85	−3.13	14.23	−7.09	14.48	−55.79	24.21	−78.25	29.04	−100.67	30.55

2.2.3. Combined Method

We combined the empirical and altitude bias correction methods (A + E) by first performing the altitude bias correction to the GOSAT SWIR XH_2O data and then conducting multilinear regression analyses between the altitude bias correction data and the retrieved parameters as described in the Section 2.1. The terms of surface pressure and altitude difference in Equation (1) were excluded because altitude bias correction was performed. ΔXH_2O values were obtained by regressing the altitude bias-corrected GOSAT data against the TCCON data. The coefficients C_0, C_1, C_2, C_3, C_4, and C_5 for all retrieved auxiliary parameters were calculated again, and the results are summarized in Table 1b.

3. Results

3.1. Comparison between the GOSAT SWIR XH_2O and TCCON XH_2O

The data period used in this study (April 2009 to December 2017) is more than three years longer than that used by Dupuy et al. [31] and Ohyama et al. [7]. The seasonal and geophysical variations of atmospheric water vapor are large among TCCON sites; therefore, we report relative XH_2O biases (in percent) instead of absolute biases (in ppm).

To estimate GOSAT SWIR XH_2O biases, we regressed the original GOSAT SWIR XH_2O land data and mixed data against TCCON data for the three collocation cases (Table 2). The total number of matched data for mixed data and land data at each site used for these calculations decrease from case 2 to case 0. The number of mixed data matches at Lauder and Four Corners, in particular, is low for cases 0 and 1; therefore, their correlation coefficients are not calculated. Maybe, these sites are far away from ocean and the retrieval is difficult due to uneven terrain including lakes near Lauder site. We obtained good linear relationships, with correlation coefficients, *R*, for data from each.

The TCCON site ranges from 0.70 to 0.99, and *R* for the pooled data from all sites ranged between 0.9 and 0.99. Total biases as well as individual site biases tended to be negative. However, owing to the very large positive biases and standard deviations and large mixed data sets for cases 1 and 2 at Dryden (40.2 $\pm$ 33.5% and 42.9 $\pm$ 37.5%, respectively), global biases of mixed data for cases 1 and 2 were positive. The results for Dryden can be explained by the high altitude (700 m) and very dry weather of the Dryden TCCON site, which is in the Mojave Desert, as well as the long distance between the TCCON site and the GOSAT observations over the Los Angeles basin, where the humidity might be relatively higher than at Dryden. Because of the finer geophysical resolution of case 0 ($0.5^\circ \times 0.5^\circ$ latitude/longitude), the station bias was $-2.3 \pm 9.0\%$ and the global bias was $-1.3 \pm 9.3\%$ for original land data, and for original mixed data, the station bias was $-1.9 \pm 7.1\%$ and the global bias was $-0.3 \pm 7.6\%$. The global biases and their standard deviations for GOSAT SWIR XH_2O data over land were $-1.4 \pm 19.1\%$ for case 1 and $-0.1 \pm 22.4\%$ for case 2, whereas the corresponding station biases were $-2.5 \pm 14.9\%$ and $-1.2 \pm 19.3\%$, respectively. The station biases and their standard deviations for GOSAT XH_2O mixed data for cases 1 and 2 were even smaller (0.5 ± 11.83 and -0.9 ± 19.8, respectively).

The slopes of the linear regression curves obtained by least-squares fitting of the original GOSAT SWIR XH_2O data to the TCCON data at each site are similar both among cases and among sites (Table 3). While the intercepts are very different, they increase from case 0 to case 2 and tend to be positive (note that the mixed data for cases 0 and 1 at Lauder and Four Corners are excluded from the regression analyses because of the small number of matched data at these sites). At most sites, the slopes are less than one and intercepts at Sodankylä, Four Corners, Bremen, and Lauder are usually negative.

Table 2. Statistical comparison between the GOSAT SWIR XH_2O and TCCON XH_2O for colocation cases 0, 1, and 2. (a) Land data and (b) mixed data. The mean bias and standard deviation (SD), total number of matched data (*N*), and correlation coefficient (*R*) are listed for each TCCON site. Also shown for each case are the total bias, SD, *N*, and *R* for all TCCON sites, and the station bias, SD, and *N*.

a) Land	**Case 0**				**Case 1**				**Case 2**			
Site	**N**	**Bias (%)**	**SD (%)**	***R***	**N**	**Bias (%)**	**SD (%)**	***R***	**N**	**Bias (%)**	**SD (%)**	***R***
Sodankylä	7	0.23	3.28	0.99	53	−7.92	15.48	0.85	114	−2.29	17.62	0.89
Bialystok	43	0.41	6.97	0.99	63	−0.66	9.42	0.98	100	−0.94	12.63	0.96
Bremen	0				5	1.39	6.29	0.99	23	−0.09	11.98	0.96
Karlsruhe	9	−3.91	8.59	0.99	63	−8.10	14.60	0.95	145	−8.84	16.15	0.85
Orléans	49	−0.64	7.08	0.99	126	0.47	10.44	0.98	269	0.72	16.22	0.95
Garmisch	39	−8.31	16.55	0.90	103	−5.24	17.96	0.93	260	4.12	32.84	0.89
Park Falls	0				30	4.52	12.10	0.97	140	7.66	32.57	0.93
Rikubetsu	9	1.71	5.84	0.99	42	5.58	12.78	0.99	91	10.03	13.94	0.97
Four Corners	7	−4.36	8.15	0.99	20	−3.09	8.50	0.99	21	−3.61	8.61	0.99
Lamont	251	1.05	6.74	0.99	469	−0.58	15.17	0.98	1046	−0.25	22.34	0.95
Tsukuba	303	−1.49	11.46	0.98	553	−1.75	16.25	0.97	706	−4.61	17.86	0.95
Dryden	400	−0.12	2.88	0.99	992	18.71	30.59	0.91	1350	23.61	34.78	0.89
JPL	489	2.38	13.19	0.97	632	0.03	22.57	0.91	897	−1.27	24.62	0.87
Caltech	818	−1.97	8.95	0.98	1648	−9.14	17.53	0.90	2003	−7.67	19.37	0.89
Saga	83	−2.03	13.35	0.96	126	−5.07	15.43	0.95	162	−5.00	17.22	0.94
Darwin	5	0.03	4.83	0.99	238	−11.06	15.47	0.86	267	−11.07	17.82	0.85
Wollongong	75	−14.67	16.81	0.94	221	−17.66	17.55	0.90	449	−17.52	18.73	0.89
Lauder	313	−4.72	9.81	0.97	386	−5.44	11.0	0.96	425	−5.22	12.21	0.95
Total	**2900**	**−1.32**	**9.33**	**0.98**	**5770**	**−1.41**	**19.06**	**0.91**	**8468**	**−0.06**	**22.41**	**0.90**
Station	**16**	**−2.27**	**9.03**		**18**	**−2.50**	**14.95**		**18**	**−1.24**	**19.31**	
b) Mixed	**Case 0**				**Case 1**				**Case 2**			
Site	**N**	**Bias (%)**	**SD (%)**	***R***	**N**	**Bias (%)**	**SD (%)**	***R***	**N**	**Bias (%)**	**SD (%)**	***R***
Sodankylä	6	0.84	2.01	0.99	17	−1.12	13.07	0.84	136	−1.64	15.27	0.91
Bialystok	0				5	0.16	7.14	0.93	99	−1.24	17.37	0.95
Bremen	13	2.33	2.27	0.99	17	1.76	2.65	0.99	39	0.59	21.31	0.96
Karlsruhe	4	−4.45	2.78	0.99	6	−4.46	2.19	0.98	53	−6.40	20.19	0.92
Orléans	9	1.27	4.42	0.99	67	0.95	16.32	0.97	169	−0.37	19.43	0.93
Garmisch	19	−8.24	13.12	0.97	42	−4.71	16.46	0.95	74	−4.00	24.39	0.89
Park Falls	395	0.23	4.49	0.99	498	−0.29	7.95	0.99	606	0.44	13.14	0.96
Rikubetsu	0				10	9.91	10.92	0.99	32	12.18	13.16	0.96
Four Corners	1	−0.49	0.00	NA	2	−8.76	8.39	NA	7	−29.52	22.77	0.93
Lamont	50	1.49	12.87	0.99	100	2.75	19.74	0.97	240	3.91	28.47	0.94
Tsukuba	119	−1.68	8.51	0.99	214	−2.28	12.69	0.98	263	−3.94	14.83	0.97
Dryden	0				159	40.16	33.52	0.91	268	42.96	37.54	0.88
JPL	42	4.19	7.39	0.97	48	1.90	9.97	0.95	79	3.49	18.22	0.87
Caltech	199	1.56	7.77	0.99	218	1.11	8.17	0.99	364	1.23	19.68	0.88
Saga	28	−6.26	18.48	0.94	42	−5.89	17.29	0.95	99	−11.66	21.31	0.94
Darwin	18	−0.69	4.79	0.99	27	−2.03	7.57	0.96	27	−2.03	7.57	0.96
Wollongong	70	−6.03	16.54	0.95	165	−7.89	18.47	0.91	273	−8.42	18.17	0.91
Lauder	3	−12.42	0.38	NA	3	−12.42	0.38	NA	13	−11.63	23.57	0.7
Total	**976**	**−0.33**	**7.57**	**0.99**	**1640**	**2.84**	**13.69**	**0.95**	**2841**	**2.78**	**19.82**	**0.91**
Station	**15**	**−1.89**	**7.06**		**18**	**0.49**	**11.83**		**18**	**−0.89**	**19.80**	

Table 3. Linear least-squares regression slope (ppm/ppm) and intercept (ppm) between original GOSAT SWIR XH_2O and TCCON data for colocation cases 0, 1, and 2.

Site	Original GOSAT for Land						Original GOSAT for Mixed					
	Case 0		Case 1		Case 2		Case 0		Case 1		Case 2	
	Slope	Intercept	Slope	Intercept	Slope	Intercept	Slope	Intercept	Slope	Intercept	Slope	Intercept
Sodankylä	1.08	−155.5	0.93	−22.1	0.94	67.7	1.02	−30.8	0.59	777.2	0.87	234.0
Bialystok	1.00	−4.3	0.98	27.4	0.95	59.4	–	–	0.79	625.5	0.90	159.6
Bremen	–	–	1.05	−82.4	1.06	−124.1	1.04	−21.1	1.03	−19.9	1.02	−48.1
Karlsruhe	0.99	−63.7	0.89	45.5	0.80	385.9	0.97	−29.6	0.96	0.3	0.82	197.7
Orléans	0.96	50.1	0.99	9.6	0.95	105.9	0.98	61.9	0.89	195.3	0.85	239.9
Garmisch	0.79	248.7	0.89	106.2	0.86	280.9	0.86	97.6	0.88	99.1	0.88	121.2
Park Falls	–	–	0.97	141.6	0.96	193.1	0.99	22.2	0.99	21.2	0.96	81.0
Rikubetsu	1.06	−67.2	1.03	47.6	1.05	102.3	–	–	0.95	168.8	0.98	217.8
Four Corners	0.95	−46.3	0.98	−34.4	0.98	−41.4	–	–	–	–	0.92	−525.9
Lamont	0.98	41.5	0.93	100.5	0.87	228.8	0.96	92.5	0.89	244.8	0.85	333.6
Tsukuba	0.93	56.4	0.91	81.1	0.85	129.2	0.95	37.0	0.91	77.2	0.88	93.3
Dryden	1.00	−2.2	0.98	308.5	0.91	761.4	–	–	1.00	600.3	0.96	407.3
JPL	0.97	104.6	0.91	169.8	0.85	275.6	0.99	93.3	0.94	176.8	0.75	634.4
Caltech	0.94	83.0	0.85	107.2	0.82	209.9	0.99	51.2	0.98	52.8	0.79	478.9
Saga	0.89	121.9	0.93	26.6	0.90	75.9	1.07	−196	0.98	−49.1	0.96	−109.9
Darwin	0.98	53.3	0.72	478.9	0.71	480.4	0.96	77.8	0.89	222.6	0.89	222.6
Wollongong	0.84	19.0	0.79	52.9	0.80	38.7	0.83	193.0	0.78	274.4	0.80	216.6
Lauder	0.98	−42.6	0.97	−36.1	0.96	−18.6	–	–	–	–	0.59	421.2

A slope of less than one between GOSAT SWIR XH_2O land data as well as mixed data and TCCON data in all cases, such as at Wollongong, Caltech, and Darwin, indicates a dry bias in the GOSAT SWIR XH_2O data despite positive intercepts [31]; XH_2O values measured by TCCON at these sites were larger than the corresponding GOSAT SWIR XH_2O values by 200 to 1500 ppm. In contrast, a wet bias is observed at Dryden due to its slope approaching one and a positive intercept associated with low humidity condition there. Maximum variability of water vapor values was observed within 30 to 35° latitude of both hemispheres; GOSAT SWIR XH_2O values at Caltech, Saga, and Wollongong ranged from 325 to 5500 ppm. In the near-polar regions as Sodankylä, GOSAT SWIR XH_2O values were low; maximum XH_2O values ranged from 3174 to 4640 ppm and maximum XH_2O values have just reached 3778 ppm at Lauder, a halfway between the equator and the South Pole. The reason for the low XH_2O values at Lauder is the rain shadow effect of the prevailing winds travelling over the Southern Alps, not the low temperatures that are experienced at Sodankylä (Figure 2). In general, the two datasets show good agreement, although with a tendency toward a dry bias.

To identify the factors accounting for GOSAT SWIR XH_2O biases, we examined the mean altitude difference between GOSAT observation points and TCCON sites for each collocation case (Table 4). The absolute values of the altitude difference depend on the collocation cases. They are larger at 13 of 18 sites for case 2 than for case 1. For case 0, the altitude differences are still large; therefore, both bias correction method (E) and bias correction method (A) will be effective even at fine resolution (0.5° × 0.5° latitude/longitude). The mean Δh values of case 1 were close to those reported by Ohyama et al. [7] when the horizontal distance between the GOSAT observation point and the ground-based instrument was within 100 km.

To investigate differences in the relationship between GOSAT observation points and TCCON site altitude for each bias correction method, we compared original and corrected GOSAT SWIR XH_2O data with TCCON data at the 18 sites for each collocation case. Then we compared and evaluated the results among the three bias correction methods.

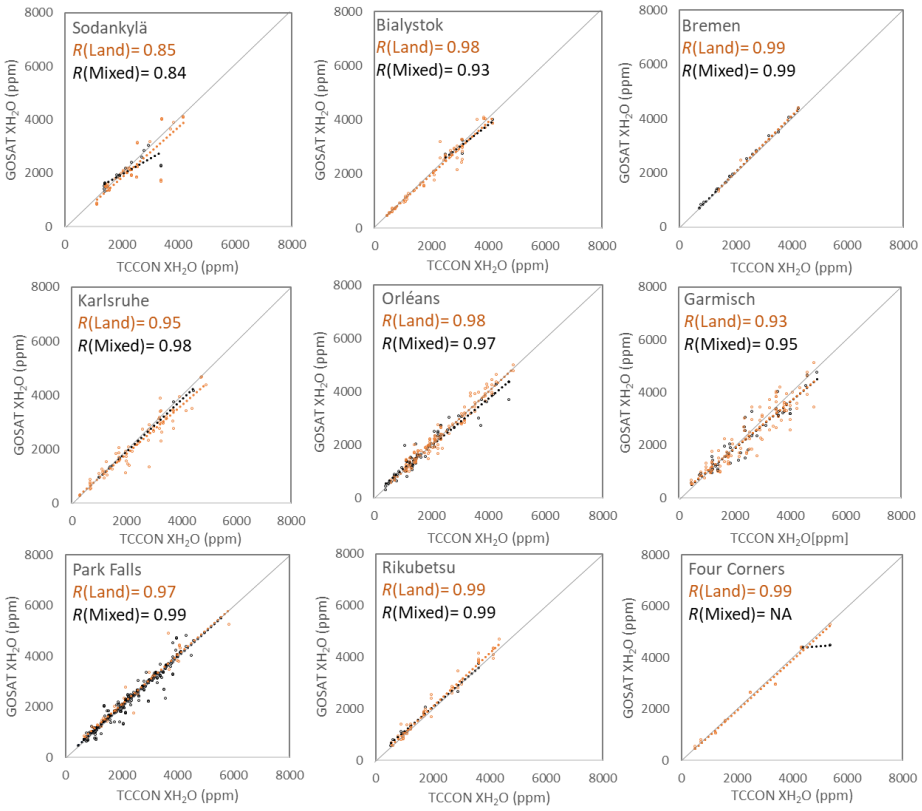

Figure 2. *Cont.*

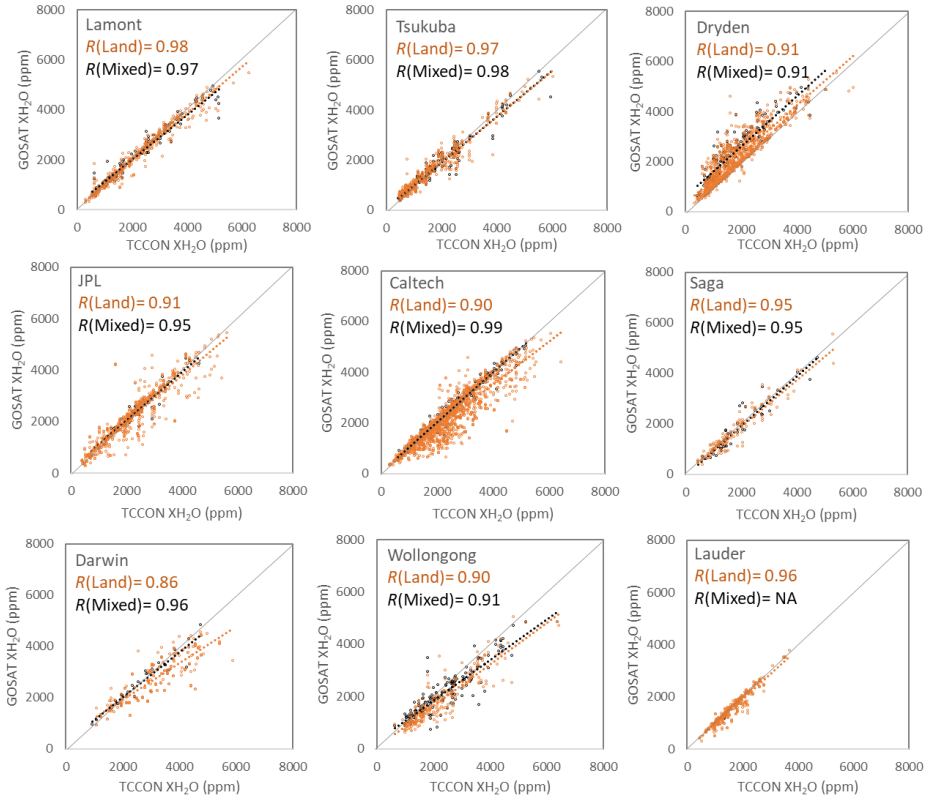

Figure 2. Scatter plots between original GOSAT SWIR XH_2O data and TCCON XH_2O data for case 1 (GOSAT data retrieved within ±1° latitude/longitude boxes centered at each TCCON site and the mean of TCCON XH_2O values within ±30 min of the GOSAT overpass time) at the 18 TCCON sites from April 2009 to December 2017. GOSAT land data (gain H) are shown by red circles and GOSAT mixed data (gain H) are shown by black circles. The regression lines fitted to the data are dotted and the solid lines show one-to-one correspondence.

Table 4. Differences in mean altitude between the GOSAT SWIR XH_2O observation point and each TCCON site for the three colocation cases. Both gain M and gain H land and mixed data were used to calculate the altitude differences.

TCCON Site (lat. (°), long. (°), alt.(m))	Case 0 Mean Δh (m)	Case 1 Mean Δh (m)	Case 2 Mean Δh (m)
Sodankylä (67.37, 26.63, 188)	−18	66	152
Białystok (53.23, 23.03, 180)	−23	−38	−54
Bremen (53.10, 8.85, 30)	−21	−19	76
Karlsruhe (49.10, 8.44, 116)	150	219	234
Orléans (47.97, 2.11, 130)	−9	−16	3
Garmisch (47.48, 11.06, 740)	49	−59	−200
Park Falls (45.94, −90.27, 440)	40	26	4
Rikubetsu (43.46, 143.77, 361)	−101	−251	−215
Four Corners (36.80, −108.48, 1643)	131	210	392
Lamont (36.60, −97.49, 320)	−9	12	34
Tsukuba (36.05, 140.12, 30)	5	30	83
Dryden (34.96, −117.88, 700)	−1	−299	−345
JPL (34.20, −118.18, 390)	−226	−92	−38
Caltech (34.14, −118.13, 237)	−29	107	91
Saga (33.24, 130.29, 8)	6	115	134
Darwin (−12.43, 130.89, 30)	5	7	9
Wollongong (−34.41, 150.88, 30)	264	342	351
Lauder (−45.05, 169.68, 370)	128	136	285

3.2. Bias Correction

Empirical bias correction of GOSAT SWIR XH_2O was first performed by the multilinear regression analysis method of Inoue et al. [59], who applied it to bias correction of GOSAT XCO_2 and XCH_4 data. Figure 3 shows scatter plots of water vapor differences between the original or bias-corrected GOSAT data and TCCON measurements versus differences in the auxiliary parameters $AOD_{1.6}$, Alb_1, Alb_2, air mass, temperature shift, altitude, and surface pressure for case 1. In brief, the results showed that both land and mixed GOSAT SWIR XH_2O data are negatively correlated with the two albedo subbands. The retrieved air mass (a function of the solar zenith angle and the satellite-viewing angle) affects both land and mixed GOSAT SWIR XH_2O data, whereas only mixed GOSAT SWIR XH_2O data are correlated with the retrieved $AOD_{1.6}$. There is a strong positive correlation between the water vapor difference in land data and surface pressure and altitude. Thus, bias correction method (E) would partly remove the altitude difference between the two measurements in land data. Similar correlation trends are observed for case 2 (not shown). For case 0, the correlation coefficients between the mixed water vapor difference data and the auxiliary parameters (excepting Alb_1, Alb_2, and $AOD_{1.6}$) are approximately zero (Figure 4).

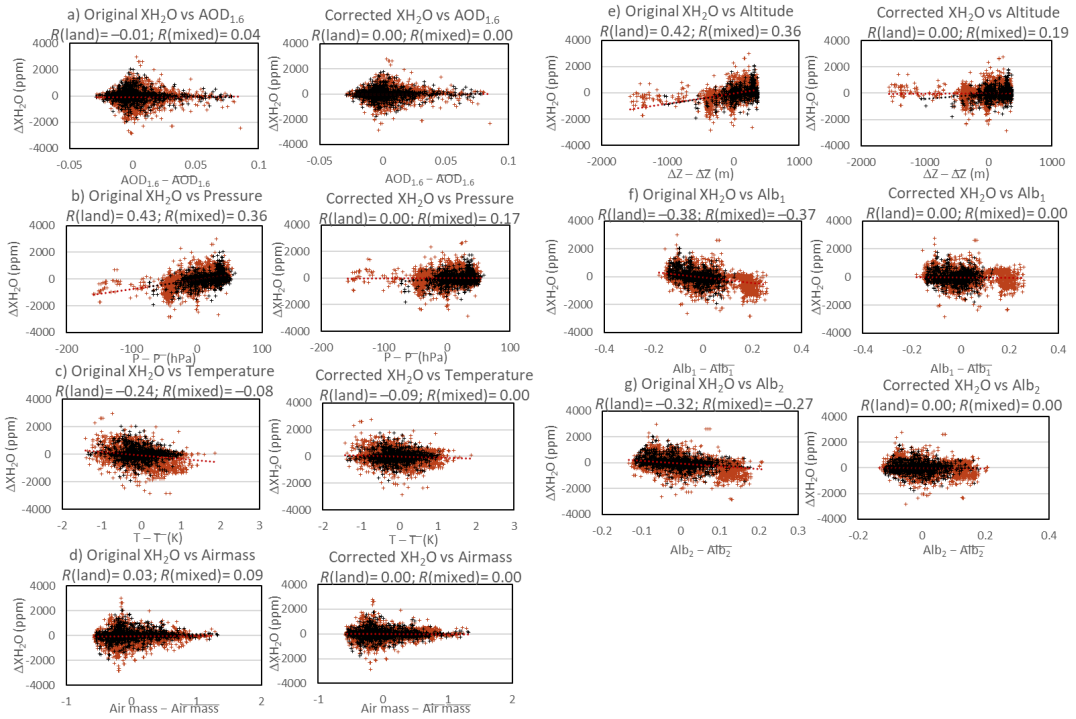

Figure 3. Scatter plots between ΔXH_2O calculated from original GOSAT SWIR XH_2O data (left panels) or from GOSAT SWIR XH_2O data corrected by bias-correction method (E) (right panels) and auxiliary parameters (**a**) $AOD_{1.6}$, (**b**) surface pressure, (**c**) temperature shift, (**d**) air mass, (**e**) altitude, (**f**) Alb_1, and (**g**) Alb_2 for case 1. Red symbols indicate GOSAT gain H land data, and black symbols indicate GOSAT gain H mixed for case 1. Red symbols indicate GOSAT gain H land data and black symbols indicate GOSAT gain H mixed data. The dotted lines are the fitted regression lines. ΔXH_2O = GOSAT XH_2O − TCCON XH_2O.

After applying the bias correction method (E) for three cases, the XH_2O bias (i.e., its absolute value) and its standard deviation of land data were decreased at some sites but those of mixed data were increased at most sites. In particular, the global bias and the station bias for case 0, for mixed XH_2O data, were increased to $0.9 \pm 9.1\%$ and $0.7 \pm 14.7\%$, respectively, after bias correction (Table 5). For land data, bias correction reduced the global bias to $0.7 \pm 9.2\%$ and station bias to $-0.4 \pm 8.6\%$. Overall, bias correction method (E) reduced the biases in land data at five and in mixed data at two

of the 18 sites. At larger temporal and spatial collocation criteria, the results were similar for case 1 (Table 6) and case 2 (Table 7).

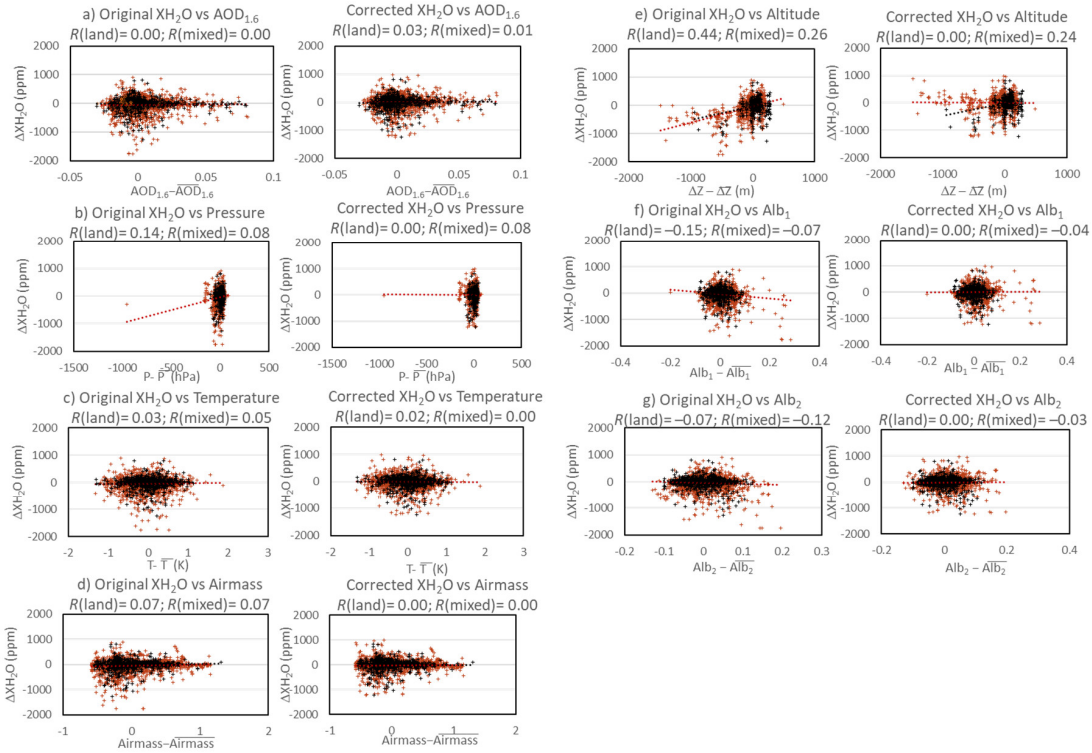

Figure 4. Scatter plots between ΔXH_2O calculated from original GOSAT SWIR XH_2O data (left panels) or from GOSAT SWIR XH_2O data corrected by bias-correction method (E) (right panels) and auxiliary parameters (**a**) $AOD_{1.6}$, (**b**) surface pressure, (**c**) temperature shift, (**d**) air mass, (**e**) altitude, (**f**) Alb_1, and (**g**) Alb_2 for case 0. Red symbols indicate GOSAT gain H land data, and black symbols indicate GOSAT gain H mixed for case 0. Red symbols indicate GOSAT gain H land data and black symbols indicate GOSAT gain H mixed data. The dotted lines are the fitted regression lines. ΔXH_2O = GOSAT XH_2O − TCCON XH_2O.

Application of bias correction method (A) showed that adjusting for the altitude difference at three cases clearly reduced bias in GOSAT SWIR XH_2O data. In case 0, the global bias changed from $-1.3 \pm 9.3\%$ to $-2.2 \pm 8.5\%$ and station bias from $-2.3 \pm 9.0\%$ to $-1.7 \pm 8.4\%$ in land data, in mixed data global bias and station bias were $-0.3 \pm 7.6\%$ and $-1.9 \pm 7.1\%$, respectively, without any bias correction. For land data, the global bias changed from $-1.4 \pm 19.1\%$ to $-2.1 \pm 16.9\%$ and reduced the station bias from $-2.5 \pm 14.9\%$ to $-2.2 \pm 14.2\%$ for case 1. The altitude bias correction also reduced the bias slightly for case 2. Bias at seven and six, for cases 1 and 2, respectively, of the 18 sites was smaller after bias correction. For mixed data, five (case 0) and six (case 1) and eight (case 2) of the 18 sites had smaller biases after bias correction. The biases at Wollongong and Lauder were also reduced for case 0, to $-5.7 \pm 14.5\%$ and $-2.1 \pm 7.8\%$ for land data and to $-3 \pm 14.6\%$ and $-3.2 \pm 0.5\%$ for mixed data.

When bias correction methods (A) and (E) were applied together as a correction method (A+E), the biases for case 1 and case 2 were mainly larger than those when method (A) was applied separately, and they tended to be positive. For land data, biases at 12 of the 18 sites, at least, were positive, and their standard deviations were mostly larger. Consequently, bias at six in land data and five in mixed data of the 18 sites was smaller for case 0. The global bias and its standard deviation of mixed data changed from $-0.3 \pm 7.6\%$ to $0.7 \pm 7.5\%$, though a small bias reduction, from $-1.3 \pm 9.3\%$ to $1.2 \pm 8.9\%$, was observed in land data after bias correction by method (A+E). There were five (case 1) and four (case 2) of the 18 sites had smaller biases after bias correction for land data. For mixed data, bias correction reduced bias at four (case 1) and seven (case 2) of the 18 sites.

Table 5. Comparison of biases and standard deviations (SD) among the three bias correction methods at the 18 TCCON sites for case 0. (E) Empirically derived bias correction, (A) altitude bias correction, and (A + E) altitude bias correction followed by empirically derived bias correction. NA, not available.

Site	Land Data								Mixed Data							
	Original		(E)		(A)		(A + E)		Original		(E)		(A)		(A + E)	
	Bias	SD	Bias	SD	Bias	SD	Bias	SD	Bias	SD	Bias	SD	Bias	SD	Bias	SD
Sodankylä	0.23	3.28	1.89	3.26	−0.15	3.54	3.18	3.35	0.84	2.01	1.79	2.07	0.23	1.92	1.08	2.07
Bialystok	0.41	6.97	2.53	8.01	−0.20	7.05	4.08	9.12	NA	NA	NA	NA	NA	NA	NA	NA
Bremen	NA	NA	NA	NA	NA	NA	NA	NA	2.33	2.27	33.92	116.11	1.68	2.28	3.15	3.19
Karlsruhe	−3.91	8.59	−2.64	8.55	1.47	7.19	5.96	9.49	−4.45	2.78	−3.89	2.96	−8.84	3.86	−7.12	3.76
Orléans	−0.64	7.08	1.16	7.46	−0.88	7.05	2.44	7.55	1.27	4.42	2.11	4.89	0.76	4.54	2.56	4.87
Garmisch	−8.31	16.55	−8.27	13.03	−8.41	13.38	−5.72	14.55	−8.24	13.12	−7.56	13.29	−7.74	11.16	−6.57	11.11
Park Falls	NA	NA	NA	NA	NA	NA	NA	NA	0.23	4.49	0.94	4.57	1.31	4.55	2.86	4.77
Rikubetsu	1.71	5.84	3.75	5.41	−0.95	5.77	2.78	5.72	NA	NA	NA	NA	NA	NA	NA	NA
Four Corners	−4.36	8.15	−3.64	5.82	−0.99	7.93	−0.26	5.97	−0.49	0.00	−0.03	0.00	−1.44	0.00	−0.32	0.0
Lamont	1.05	6.74	3.38	7.21	0.75	6.78	4.59	7.60	1.49	12.87	1.71	12.89	1.42	12.39	2.00	12.91
Tsukuba	−1.49	11.46	1.48	12.25	−1.21	11.48	3.94	12.69	−1.68	8.51	0.05	8.86	−1.95	8.47	0.50	8.77
Dryden	−0.12	2.88	1.75	3.42	−0.16	2.95	3.27	3.45	NA	NA	NA	NA	NA	NA	NA	NA
JPL	2.38	13.19	3.79	12.56	−4.96	11.75	−2.01	11.67	4.19	7.39	5.22	7.44	−5.38	6.56	−3.32	6.79
Caltech	−1.97	8.95	−0.02	8.48	2.66	7.94	0.07	7.82	1.56	7.77	2.13	7.77	−1.98	7.16	−0.75	7.48
Saga	−2.03	13.35	0.07	13.87	−1.83	13.41	2.00	14.34	−6.26	18.48	−5.41	18.52	−6.24	18.52	−4.32	18.68
Darwin	0.03	4.83	0.15	4.77	0.18	5.16	1.24	4.65	−0.69	4.80	0.12	4.87	−0.54	4.75	1.03	5.11
Wollongong	−14.67	16.81	−8.51	13.44	−5.68	14.52	−2.43	15.27	−6.03	16.54	−5.69	15.88	−2.98	14.63	−2.18	14.29
Lauder	−4.72	9.81	−3.01	10.20	−2.13	7.84	1.54	8.30	−12.47	0.38	−14.56	0.19	−3.18	0.47	−6.22	0.44
Total	**−1.32**	**9.33**	**0.72**	**9.22**	**−2.23**	**8.50**	**1.16**	**8.87**	**−0.33**	**7.57**	**0.85**	**9.13**	**−0.84**	**7.24**	**0.66**	**7.47**
Station	**−2.28**	**9.03**	**−0.39**	**8.61**	**−1.74**	**8.36**	**1.54**	**8.85**	**−1.89**	**7.06**	**0.72**	**14.69**	**−2.33**	**6.75**	**−1.17**	**6.95**

Table 6. Comparison of biases and standard deviations (SD) among the three bias correction methods at the 18 TCCON sites for case 1. (E) Empirically derived bias correction, (A) altitude bias correction, and (A + E) altitude bias correction followed by empirically derived bias correction.

Site	Land Data								Mixed Data							
	Original		(E)		(A)		(A + E)		Original		(E)		(A)		(A + E)	
	Bias	SD	Bias	SD	Bias	SD	Bias	SD	Bias	SD	Bias	SD	Bias	SD	Bias	SD
Sodankylä	−7.92	15.48	−5.25	15.37	−6.04	15.65	−2.85	15.74	−1.12	13.07	2.40	14.38	−0.39	13.39	1.76	14.10
Bialystok	−0.66	9.42	3.56	9.91	−1.66	9.16	4.27	10.94	0.16	7.14	−2.56	6.88	−1.90	7.18	−1.74	7.18
Bremen	1.39	6.29	3.98	5.27	0.96	6.25	4.33	5.99	1.76	2.65	3.79	6.37	1.11	2.63	3.26	4.35
Karlsruhe	−8.10	14.60	−5.10	14.89	−2.20	15.38	2.13	16.23	−4.46	2.19	2.35	3.26	−4.91	2.16	−1.54	2.37
Orléans	0.47	10.44	3.49	10.84	−0.04	10.25	3.90	10.74	0.95	16.32	6.32	17.52	0.51	16.22	3.13	16.92
Garmisch	−5.24	17.96	−3.29	16.14	−8.17	15.34	−4.10	16.47	−4.71	16.46	−3.15	17.37	−6.47	15.55	−4.77	15.13
Park Falls	4.52	12.10	7.06	15.33	2.65	12.97	9.68	15.78	−0.29	7.95	1.71	8.69	1.07	8.52	3.20	8.64
Rikubetsu	5.58	12.78	9.50	12.71	−0.66	11.76	3.79	11.86	9.91	10.92	12.1	12.42	−0.90	9.22	−1.11	8.26
Four Corners	−3.09	8.50	0.19	8.74	1.67	9.65	3.08	8.55	−8.76	8.39	−6.93	9.71	−6.99	5.68	−5.68	6.22
Lamont	−0.58	15.17	3.64	16.14	−0.05	15.26	5.62	16.22	2.75	19.74	1.07	19.14	1.85	20.05	2.85	19.63
Tsukuba	−1.75	16.25	2.97	17.17	−0.84	16.47	5.95	17.96	−2.28	12.69	0.91	15.53	−1.94	12.74	1.29	13.45
Dryden	18.71	30.59	25.04	26.98	8.33	23.31	14.41	23.40	40.16	33.52	21.81	36.52	15.69	27.32	11.35	28.56
JPL	0.03	22.57	3.63	25.10	−4.16	20.55	0.19	21.57	1.90	9.97	4.09	10.08	−6.28	7.56	−3.54	7.82
Caltech	−9.14	17.53	−5.98	16.08	−6.61	15.40	−2.68	14.97	1.11	8.17	−7.66	11.13	−1.98	7.48	−3.49	8.39
Saga	−5.07	15.43	−0.63	16.44	−2.56	15.12	2.80	16.28	−5.89	17.30	−3.95	18.52	−4.37	17.85	−1.88	18.19
Darwin	−11.06	15.47	−8.88	15.54	−10.83	15.56	−7.92	15.75	−2.03	7.57	0.91	11.39	−2.02	7.58	0.37	8.61
Wollongong	−17.66	17.55	−10.24	17.60	−5.95	18.34	−2.14	19.17	−7.89	18.47	−5.98	18.02	−4.75	17.01	−2.93	16.76
Lauder	−5.44	11.00	−1.67	9.55	−2.53	9.62	2.78	10.17	−12.42	0.38	−18.84	0.23	−3.13	0.47	−8.83	0.31
Total	**−1.41**	**19.06**	**2.75**	**18.39**	**−2.12**	**16.89**	**2.75**	**17.29**	**2.84**	**13.69**	**1.50**	**15.12**	**0.46**	**12.95**	**1.53**	**13.34**
Station	**−2.50**	**14.95**	**1.22**	**14.99**	**−2.15**	**14.22**	**2.40**	**14.88**	**0.49**	**11.83**	**0.47**	**13.18**	**−1.43**	**11.03**	**−0.46**	**11.38**

Table 7. Comparison of biases and standard deviations (SD) among the three bias correction methods at 18 the TCCON sites for case 2. (E) Empirically derived bias correction, (A) altitude bias correction, and (A + E) altitude bias correction followed by empirically derived bias correction.

Site	Land Data								Mixed Data							
	Original		(E)		(A)		(A + E)		Original		(E)		(A)		(A + E)	
	Bias	SD	Bias	SD	Bias	SD	Bias	SD	Bias	SD	Bias	SD	Bias	SD	Bias	SD
Sodankylä	−2.29	17.62	2.46	17.95	−0.79	17.95	4.21	18.97	−1.64	15.27	−1.64	15.27	−2.76	14.96	1.73	16.10
Bialystok	−0.94	12.63	2.16	13.3	−2.25	12.45	3.74	13.45	−1.24	17.37	−0.16	16.39	−2.86	17.28	−0.48	16.27
Bremen	−0.09	11.98	3.73	10.79	4.25	13.19	8.49	13.37	0.59	21.31	2.16	23.20	3.52	23.02	6.79	24.39
Karlsruhe	−8.84	16.15	−6.82	17.94	−2.46	17.05	1.49	17.66	−6.40	20.19	−5.24	20.40	−3.38	20.15	−0.79	19.96
Orléans	0.72	16.22	3.37	17.07	0.79	16.31	5.24	17.43	−0.37	19.43	1.32	19.67	−0.51	18.86	2.49	18.58
Garmisch	4.12	32.84	3.63	26.67	−4.11	29.59	0.93	32.08	−4.00	24.39	−4.10	24.4	−12.53	21.92	−10.7	22.25
Park Falls	7.66	32.57	9.96	34.38	5.43	32.19	15.19	36.06	0.44	13.14	1.05	13.54	1.03	12.96	3.76	13.39
Rikubetsu	10.03	13.94	13.28	15.32	14.33	17.55	20.16	17.37	12.18	13.16	11.65	12.73	14.47	18.14	15.47	19.21
Four Corners	−3.61	8.61	−0.47	17.36	2.04	9.56	5.20	9.99	−29.52	22.77	−42.18	24.36	−20.48	29.35	−26.71	26.22
Lamont	−0.25	22.34	3.25	23.14	1.06	22.34	6.78	23.69	3.91	28.47	4.10	28.22	2.48	28.33	4.81	28.57
Tsukuba	−4.61	17.86	−0.68	18.81	−2.42	17.56	4.49	19.35	−3.94	14.83	−1.74	16.01	−3.32	14.71	1.06	15.99
Dryden	23.61	34.78	29.08	32.19	11.48	32.33	17.64	32.33	42.96	37.54	39.29	41.07	22.66	32.25	23.07	35.28
JPL	−1.27	24.62	1.20	26.02	−3.88	22.41	0.28	24.12	3.49	18.22	5.71	19.81	−3.18	16.79	0.73	18.35
Caltech	−7.67	19.37	−4.91	18.00	−4.95	20.77	−1.09	20.11	1.23	19.68	−0.70	20.65	−1.85	19.32	−1.13	19.65
Saga	−5.00	17.22	−2.03	18.08	−2.74	16.85	3.29	18.07	−11.66	21.31	−10.33	22.66	−9.26	20.38	−5.94	21.26
Darwin	−11.07	17.82	−8.86	17.79	−10.59	17.90	−7.42	18.06	−2.03	7.57	−0.19	9.35	−2.02	7.58	0.89	9.09
Wollongong	−17.52	18.76	−10.53	18.73	−6.18	19.60	−1.95	20.59	−8.42	18.17	−7.37	17.15	−5.38	16.55	−2.78	16.32
Lauder	−5.22	12.21	−2.28	10.55	−2.64	10.54	3.10	11.89	−11.63	23.57	−12.89	16.60	−7.31	19.31	−5.98	15.95
Total	**−0.06**	**22.41**	**3.43**	**21.88**	**−0.59**	**22.01**	**4.50**	**22.71**	**2.78**	**19.82**	**2.90**	**20.44**	**0.55**	**18.94**	**2.99**	**19.58**
Station	**−1.24**	**19.31**	**1.97**	**19.67**	**−0.20**	**19.23**	**4.99**	**20.26**	**−0.89**	**19.8**	**−1.18**	**20.08**	**−1.70**	**19.55**	**0.35**	**19.82**

4. Discussion

In the bias correction method (E), Figures 3 and 4 present correlations between retrieved GOSAT SWIR XH_2O values and simultaneously derived auxiliary parameters. The correlation between mixed XH_2O data and $AOD_{1.6}$ is strong for cases 1 and 2 but relatively weak for case 0. As well a negative correlation of land GOSAT SWIR XH_2O data with temperature is observed in cases 1 and 2, and it changes to positive correlation in case 0. There are significant negative correlations of both land and mixed GOSAT SWIR XH_2O data with albedo at 6255 cm^{-1} and 13,200 cm^{-1}. However, under more rigorous collocation criteria of case 0, bias correction of both land and mixed GOSAT SWIR XH_2O data is less effective in relation to albedo compared with cases 1 and 2. Thus, changes in albedo may affect GOSAT SWIR XH_2O biases. These correlations with albedo need more detailed study in the future. In case 0, correlations between retrieved GOSAT SWIR XH_2O values and simultaneously derived auxiliary parameters are weak excepting pressure and altitude. Then significant bias is reduced for land data by removing these correlations. The effectiveness of bias correction method (E) for reducing bias in GOSAT SWIR XH_2O data was small compared with the method's effectiveness for XCO_2 and XCH_4, as reported by Inoue et al. [59]. The reason might be high variability of XH_2O compared with XCO_2 or XCH_4.

In particular, bias was removed at Wollongong and Lauder approximately 60% after applying the bias correction method (A). Further, for case 0, although not for cases 1 or 2, more than 75% of the bias was removed for land data at Four Corners. The reason maybe comes from large altitude discrepancies in these sites between the GOSAT SWIR XH_2O observation point and TCCON site (Table 4). The standard deviations obtained with bias correction method (A) were smaller than those obtained with bias correction method (E). Therefore, the bias reductions by bias correction method (A) are meaningful.

Moreover, both the global bias and the station bias also became positive after bias correction. This result means that the GOSAT SWIR XH_2O data were adjusted so that they exceeded the TCCON data. The combined (A + E) method aimed to combine advantages of method (A) and method (E). However, their large global bias and station bias made this method ineffective.

To evaluate which bias correction method was the best at bias reduction, we compared the results for each of the three collocation cases individually (Tables 5–7). Bias correction method (A) yielded the smallest bias values for both land data and mixed data. For case 0 (Table 5), the mean bias of GOSAT SWIR XH_2O differences among TCCON sites ranged from −8.4% to 2.7% and their standard deviations ranged from 3% to 14.5% for land data, and for mixed data, the mean biases ranged from −8.8% to 1.7% and the standard deviations from 0% to 18.5%. The bias correction method (E) had larger values of the mean bias from −8.5% to 3.8% and their standard deviations from 3.3% to 13.9% for land data, and for mixed data, the mean biases ranged from −14.6% to 33.9% and the standard deviations from 0% to 116.1%. While in the correction method (A+E), the mean bias ranged from −5.7% to 6% and their standard deviations ranged from 3.4% to 15.3% for land data; and for mixed data, the mean biases ranged from −7.1% to 3.2% and the standard deviations from 0% to 18.7%. Similar trends were obtained with three bias correction methods for case 1 (Table 6) and case 2 (Table 7). Ohyama et al. [7] reported a station bias between GOSAT SWIR XH2O and TCCON data of 0.63 ± 13.4%, close to our case 1 result (−2.15 ± 14.2%). The discrepancies between their results and ours are probably attributable to different GOSAT data versions, time periods, and collocation distances between the studies.

In general, three bias correction methods get benefit from reducing spatial and temporal variability of XH_2O by geophysical collocation criteria. For all three collocation cases, bias correction method (A) successfully reduced GOSAT SWIR XH_2O biases and their standard deviations, whereas bias correction method (E) was ineffective because biases for mixed data increased and it had the largest standard deviations. Bias correction method (A + E) was also less effective because it yielded large biases and standard deviations for both land and mixed data. Therefore, altitude differences between GOSAT observation points and TCCON sites appear to be the main cause of bias. Thus, by minimizing

the altitude differences, systematic biases might be reduced. In summary, among the three methods evaluated bias correction method (A) was the most effective and bias correction method (E) was least effective.

All three bias correction techniques improved the accuracy of GOSAT SWIR XH_2O data (Tables 5–7). However, bias correction was not effective at minimizing biases and standard deviations without also increasing the resolution of collocation criteria (the bias reduction from case 2 to case 0 was approximately 50%), probably because of the high variability of XH_2O in space and time.

To assess the agreement between the GOSAT SWIR XH_2O data before and after bias correction and TCCON data, we examined linear correlations between them (Figure 5). In general, correlations between GOSAT SWIR XH_2O and TCCON data were high. For original GOSAT SWIR XH_2O data, R ranged from 0.89 to 0.99, depending on the collocation case, indicating strong, positive (direct) correlations, particularly for mixed data. The agreement between GOSAT and TCCON measurements improved after bias correction; R increased to 0.91−0.93 for case 2, to 0.93−0.97 for case 1, and for case 0, R approached 0.99. Thus, bias correction reduced data scatter and improved both the accuracy and precision of GOSAT SWIR XH_2O data. In collocation cases, bias correction method (A + E) reduced the scatter more than either bias correction method (E) or (A) applied alone except case 0.

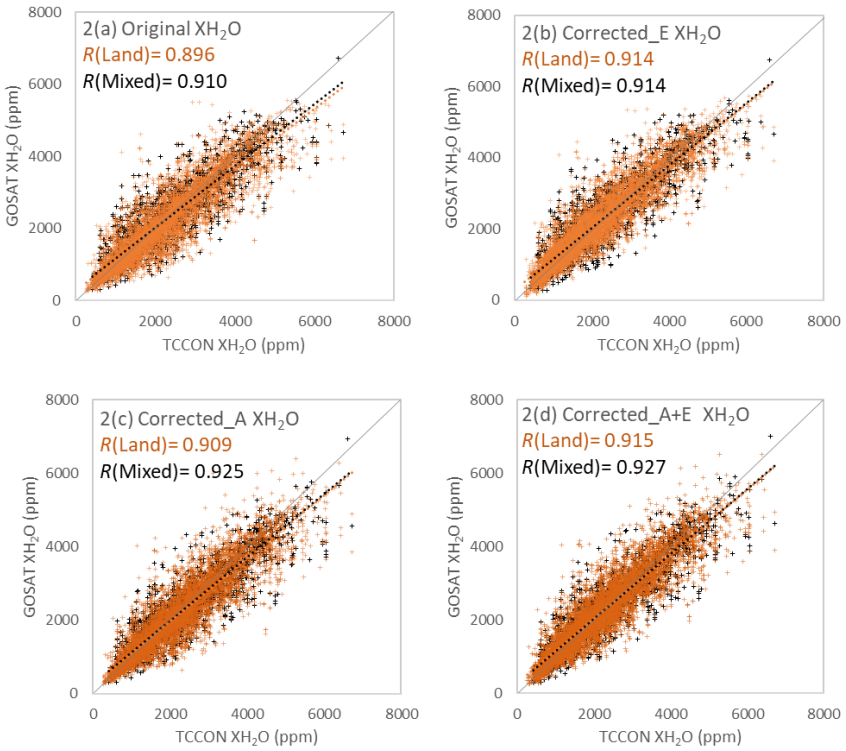

Figure 5. *Cont.*

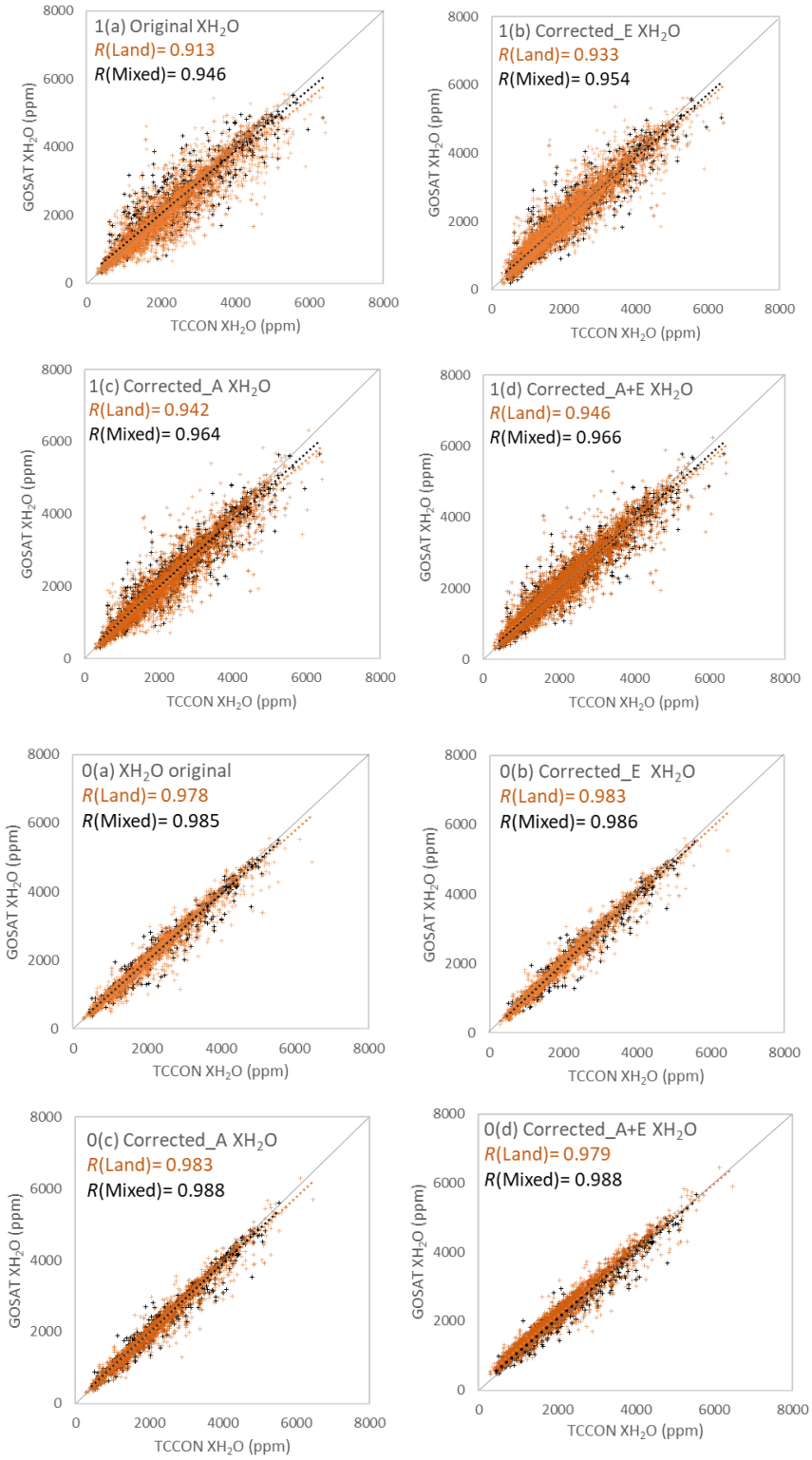

Figure 5. Correlations between GOSAT SWIR XH_2O and TCCON XH_2O for case 2 (**a**–**d**), case 1 (**a**–**d**), and case 0 (**a**–**d**). (**a**) Original GOSAT SWIR XH_2O and TCCON XH_2O, (**b**) GOSAT SWIR XH_2O corrected by bias correction method (E) and TCCON XH_2O, (**c**) GOSAT SWIR XH_2O corrected by bias correction method (A) and TCCON XH_2O, and (**d**) GOSAT SWIR XH_2O corrected by bias correction method (A + E) and TCCON XH_2O. Red symbols indicate GOSAT gain H land data and black symbols indicate GOSAT gain H mixed data. The dotted lines are the fitted regression lines and the solid lines show one-to-one correspondence.

5. Conclusions

We applied an altitude bias correction method and an empirically derived bias correction method as well as the combination of the two methods to GOSAT SWIR XH_2O data. In addition, owing to the high spatial and temporal variabilities of XH_2O, we compared the bias correction methods for three sets of collocation criteria. Evaluation of the results of each bias correction method showed that the altitude bias correction method yields consistently better results than the empirically derived bias correction method and the combination of the two methods since the bias from the altitude difference between TCCON sites and GOSAT observation points was resolved. The lowest bias of the altitude bias correction method is obtained at case 0. In land data, global bias is $-2.2 \pm 8.5\%$ and station bias is $-1.7 \pm 8.4\%$. In mixed data, global bias and station bias are $-0.8 \pm 7.2\%$ and $-2.3 \pm 6.8\%$, respectively, after bias correction. For all three collocation cases, the mixed data were more scattered after application of the empirically derived bias correction method. Thus, the multilinear regression analysis results showed that GOSAT SWIR XH_2O bias correction by the empirical method of mixed data, in particular, is ineffective. Bias in GOSAT SWIR XH_2O data is mainly attributable to altitude differences between the TCCON sites and GOSAT observation points and to the high spatial and temporal variability of XH_2O. Our results confirmed that the geophysical collocation criteria used for GOSAT SWIR XH_2O bias correction greatly affect the results. In addition, GOSAT SWIR XH_2O data are correlated mainly with the retrieved albedo and air mass (a function of the solar zenith angle and the satellite-viewing angle). However, only the mixed data are correlated with the retrieved AOD at 1.6 μm, whereas land data are correlated strongly with surface pressure and altitude of GOSAT observation point.

The correlation coefficient R, which ranged from 0.91 to 0.99 after bias correction, demonstrated that corrected GOSAT SWIR XH_2O data are very strongly correlated with TCCON data.

Besides that, the imperfect retrieval algorithms of GOSAT data as well potential bias from TCCON might also contribute to GOSAT SWIR XH_2O total bias.

In future, the distribution of relative errors in GOSAT SWIR XH_2O data should be checked. Besides, the bias correction method (E) would be tested the quality of the bias correction by a separate dataset which is not used to define the regression coefficients. Then it would be hoped that this bias correction is applicable not only for the vicinity of the TCCON sites, but also for the entire global coverage.

Author Contributions: T.T.N.T. performed all bias corrections for XH_2O presented in this paper, produced the figures and tables and wrote the entire paper. H.O. was responsible for data in the Appendix A. I.M. took extensive part in the data analysis and the writing and review of this paper. O.U. participated in the writing and review of the paper. Other authors are members of the TCCON contributed to the acquisition, processing, and delivery of the TCCON data products for the sites included in this study. All authors provided feedback on the data analysis and the writing of this manuscript.

Funding: This research was supported in part by the GOSAT project.

Acknowledgments: The GOSAT SWIR XH_2O was extracted from GOSAT Level 2 product. The GOSAT project is promoted jointly by JAXA, NIES, and the Ministry of the Environment, Japan. The TCCON data were obtained from the TCCON Data Archive, operated by the California Institute of Technology.

Conflicts of Interest: The authors declare no conflicts of interest.

Appendix A

Table A1. Coordinates of TCCON sites and nearby radiosonde launch sites.

TCCON Sites (Lat (°), Lon (°), Alt. (m))	Radiosonde Sites (Lat (°), Lon (°), Alt. (m))	Differences between the TCCON and Radiosonde Sites	
		Horizontal Distances (km)	ΔAlt. (m)
Sodankylä (67.37, 26.63, 188)	Sodankylä (67.37, 26.65, 178)	0.9	10
Białystok (53.23, 23.03, 180)	Legionowo (52.40, 20.97, 96)	166.6	84
Bremen (53.10, 8.85, 30)	Bergen (52.82, 9.93, 70)	78.8	−40
Karlsruhe (49.10, 8.44, 116)	Stuttgart (48.83, 9.20, 315)	63.2	−199
Orléans (47.97, 2.11, 130)	Trappes (48.77, 2.00, 168)	89.4	−38
Garmisch (47.48, 11.06, 740)	Altenstadt (47.83, 10.87, 738)	41.5	2
Park Falls (45.94, −90.27, 440)	Green Bay (44.48, −88.13, 214)	233.6	226
Four Corners (36.80, −108.48, 1643)	Grand Junction (39.12, −108.52, 1474)	258.3	169
Lamont (36.60, −97.49, 320)	Lamont (36.62, −97.48, 315)	2.4	5
Tsukuba (36.05, 140.12, 30)	Tateno (36.05, 140.13, 31)	0.9	−1
JPL (34.20, −118.18, 390)	Vandenberg AFB (34.75, −120.57, 100)	227.7	290
Saga (33.24, 130.29, 8)	Fukuoka (33.58, 130.38, 15)	38.8	−7
Darwin (−12.43, 130.89, 30)	Darwin (−12.43, 130.87, 29)	2.2	1
Wollongong (−34.41, 150.88, 30)	Williamtown (−32.82, 151.83, 9)	197.7	21
Lauder (−45.05, 169.68, 370)	Invercargill (−46.42, 168.32, 4)	185.5	366
Rikubetsu (43.46, 143.77, 361)	Kushiro (42.95, 144.44, 14)	78.6	347
Dryden (34.96, −117.88, 700)	Edwards AFB (34.92, −117.90, 705)	4.8	−5

Table A2. Rates of change of integrated water vapor (IWV) with respect to height (% per 100 m) for each TCCON site.

TCCONSites	Jan	Feb	Mar	Apr	May	Jun	Jul	Aug	Sep	Oct	Nov	Dec
Sodankylä	3.8	3.9	4.3	4.1	3.9	3.7	3.8	4.0	4.2	4.0	4.0	4.1
Bialystok	3.7	3.9	4.1	4.0	3.8	3.8	3.7	3.8	4.0	4.1	3.9	3.9
Bremen	4.1	4.1	4.5	4.1	3.9	4	3.8	3.9	4.1	4.1	4.2	4.1
Karlsruhe	4.1	4.1	4.3	4.1	4.0	3.9	3.8	3.9	4.1	4.0	4.0	3.9
Orléans	4.3	4.3	4.5	4.2	4.1	4.0	3.9	3.9	4.1	4.1	4.2	4.2
Garmisch	4.1	4.1	4.5	4.3	4.1	4.0	4.0	4.0	4.3	4.2	4.2	4.0
ParkFalls	3.3	3.6	3.6	3.3	3.7	3.8	3.9	4.1	4.1	3.7	3.7	3.6
Rikubetsu	4.6	4.5	4.0	3.8	3.5	3.5	3.4	3.4	3.7	4.0	4.3	4.2
FourCorners	3.7	4.2	3.9	3.7	3.5	3.2	3.2	3.4	3.5	3.7	4.0	3.8
Lamont	3.6	4.0	4.1	4.1	4.3	4.1	3.6	3.7	3.6	3.8	4.1	3.7
Tsukuba	4.2	3.6	3.6	4.0	3.9	3.6	3.5	3.6	3.6	3.6	4.0	3.9
Dryden	3.5	4.5	4.8	4.4	4.3	4.1	3.4	3.6	3.5	4.1	4.4	4.2
JPL	3.9	4.5	4.5	4.5	4.4	4.2	3.7	4.0	4.0	4.4	4.5	4.2
Saga	4.2	3.6	3.6	3.8	3.7	3.5	3.5	3.4	3.6	3.9	3.9	4.1
Darwin	3.6	3.7	3.7	3.9	3.8	4.1	4.0	4.8	4.6	4.2	4.0	3.7
Wollongong	4.1	4.0	4.3	4.4	4.5	4.5	4.5	4.7	4.7	4.4	4.3	4.0
Lauder	3.9	3.9	3.9	4.0	4.2	4.4	4.5	4.6	4.3	4.2	3.9	3.9

References

1. Starr, D.O.; Melfi, S.H. The Role of Water Vapor in Climate—A Strategic Research Plan for the Proposed GEWEX Water Vapor Project (GVaP). In Proceedings of the NASA Conference Publication 3120, Tidewater Inn, Easton, MD, USA, 30 October–1 November 1990.
2. Jacob, D. The role of water vapor in the atmosphere. A short overview from a climate modeller's point of view. *Phys. Chem. Earth Part A Solid Earth Geod.* **2001**, *26*, 523–527. [CrossRef]
3. Thies, B.; Bendix, J. Review Satellite based remote sensing of weather and climate: Recent achievements and future perspectives. *Meteorol. Appl.* **2011**, *18*, 262–295. [CrossRef]
4. *Water Vapor in the Climate System*; AGU Special Report; The American Geophysical Union: Washington, DC, USA, 2009; ISBN 0-87590-865-9.
5. Alexander, L.; William, B.; Luca, B.; Claire, E.B.; Jörg, B.; Xavier, C.; Reik, V.D.; Darren, G.; Alexander, G.; Thomas, K.; et al. Validation practices for satellite-based Earth observation data across communities. *Rev. Geophys.* **2017**, *55*, 779–817. [CrossRef]
6. Chazette, P.; Marnas, F.; Totems, J.; Shang, X. Comparison of IASI water vapor retrieval with H_2O-Raman lidar in the framework of the Mediterranean HyMeX and ChArMEx programs. *Atmos. Chem. Phys.* **2014**, *14*, 9583–9596. [CrossRef]
7. Ohyama, H.; Kawakami, S.; Shiomi, K.; Morino, I.; Uchino, O. Intercomparison of XH_2O Data from the GOSAT TANSO-FTS (TIR and SWIR) and Ground-Based FTS Measurements: Impact of the Spatial Variability of XH_2O on the Intercomparison. *Remote Sens.* **2017**, *9*, 64. [CrossRef]
8. Schneider, A.; Borsdorff, T.; Brugh, J.; Hu, H.; Landgraf, J. A full-mission dataset of H_2O and HDO columns from SCIAMACHY 2.3 μm reflectance. *Atmos. Meas. Tech.* **2018**, *11*, 3339–3350. [CrossRef]
9. John, V.O.; Holl, G.; Allan, R.P.; Buehler, S.A.; Parker, D.E.; Soden, B.J. Clear-sky biases in satellite infrared estimates of upper tropospheric humidity and its trends. *J. Geophys. Res.* **2011**, *116*, D14108. [CrossRef]
10. John, R.L.; Gregory, E.G. The "Clear-Sky Bias" of TOVS Upper-Tropospheric Humidity. *J. Clim.* **2000**, *13*, 4034–4041. [CrossRef]
11. Hegglin, M.I.; Plummer, D.A.; Shepherd, T.G.; Scinocca, J.F.; Anderson, J.; Froidevaux, L.; Funke, B.; Hurst, D.; Rozanov, A.; Urban, J.; et al. Vertical structure of stratospheric water vapour trends derived from merged satellite data. *Nat. Geosci.* **2014**, *7*, 768–776. [CrossRef]
12. Kuze, A.; Suto, H.; Nakajima, M.; Hamazaki, T. Thermal and near infrared sensor for carbon observation Fourier-transform spectrometer on the Greenhouse Gases Observing Satellite for greenhouse gases monitoring. *Appl. Opt.* **2009**, *48*, 6716–6733. [CrossRef]
13. Wunch, D.; Toon, G.C.; Blavier, J.-F.L.; Washenfelder, R.A.; Notholt, J.; Connor, B.J.; Griffith, D.W.T.; Sherlock, V.; Wennberg, P.O. The total carbon column observing network. *Philos. Trans. R. Soc. A* **2011**, *369*, 2087–2112. [CrossRef] [PubMed]
14. Dunya, A.; Alain, S.; Philippe, K.; Olivier, B.; Stefan, N.; Slimane, B.; Abdenour, I.; Mustapha, M.; Chantal, C. Comparison of total water vapour content in the Arctic derived from GNSS, AIRS, MODIS and SCIAMACHY. *Atmos. Meas. Tech.* **2018**, *11*, 2949–2965. [CrossRef]
15. Buehler, S.A.; Östman, S.; Melsheimer, C.; Holl, G.; Eliasson, S.; John, V.O.; Blumenstock, T.; Hase, F.; Elgered, G.; Raffalski, U.; et al. A multi-instrument comparison of integrated water vapour measurements at a high latitude site. *Atmos. Chem. Phys.* **2012**, *12*, 10925–10943. [CrossRef]
16. Pałm, M.; Melsheimer, C.; Noel, S.; Heise, S.; Notholt, J.; Burrows, J.; Schrems, O. Integrated water vapor above Ny Ålesund, Spitsbergen: A multi-sensor intercomparison. *Atmos. Chem. Phys.* **2010**, *10*, 1215–1226. [CrossRef]
17. Niell, A.E.; Coster, A.J.; Solheim, F.S.; Mendes, V.B.; Toor, P.C.; Langley, R.B.; Upham, C.A. Comparison of measurements of atmospheric wet delay by radiosonde, water vapor radiometer, GPS, and VLBI. *J. Atmos. Ocean. Technol.* **2001**, *80*, 830–850. [CrossRef]
18. Sussmann, R.; Borsdorff, T.; Rettinger, M.; Camy-Peyret, C.; Demoulin, P.; Duchatelet, P.; Mahieu, E.; Servais, C. Harmonized retrieval of column-integrated atmospheric water vapor from the FTIR network—First examples for long-term records and station trends. *Atmos. Chem. Phys.* **2009**, *9*, 8987–8999. [CrossRef]

19. Vogelmann, H.; Sussmann, R.; Trickl, T.; Borsdorff, T. Intercomparison of atmospheric water vapor soundings from the differential absorption lidar (DIAL) and the solar FTIR system on Mt. Zugspitze. *Atmos. Meas. Tech.* **2011**, *4*, 835–841. [CrossRef]
20. Vogelmann, H.; Sussmann, R.; Trickl, T.; Reichert, A. Spatiotemporal variability of water vapor investigated using lidar and FTIR vertical soundings above the Zugspitze. *Atmos. Chem. Phys.* **2015**, *15*, 3135–3148. [CrossRef]
21. Sapucci, L.F.; Machado, L.A.T.; Monico, J.F.G.; Plana Fattori, A. Intercomparison of integrated water vapor estimates from multisensors in the amazonian region. *J. Atmos. Ocean. Technol.* **2007**, *24*, 1880–1894. [CrossRef]
22. Van Malderen, R.; Brenot, H.; Pottiaux, E.; Beirle, S.; Hermans, C.; De Mazière, M.; Wagner, T.; De Backer, H.; Bruyninx, C. A multi-site intercomparison of integrated water vapour observations for climate change analysis. *Atmos. Meas. Tech.* **2014**, *7*, 2487–2512. [CrossRef]
23. Bedka, S.; Knuteson, R.; Revercomb, H.; Tobin, D.; Turner, D. An assessment of the absolute accuracy of the Atmospheric Infrared Sounder v5 precipitable water vapor product at tropical, midlatitude, and arctic ground-truth sites: September 2002 through August 2008. *J. Geophys. Res.* **2010**, *115*, D17310. [CrossRef]
24. Weaver, D.; Strong, K.; Walker, K.A.; Sioris, C.; Schneider, M.; McElroy, C.T.; Vömel, H.; Sommer, M.; Weigel, K.; Rozanov, A.; et al. Comparison of ground-based and satellite measurements of water vapour vertical profiles over Ellesmere Island, Nunavut. *Atmos. Meas. Tech. Discuss.* **2018**. [CrossRef]
25. Morino, I.; Uchino, O.; Inoue, M.; Yoshida, Y.; Yokota, T.; Wennberg, P.O.; Toon, G.C.; Wunch, D.; Roehl, C.M.; Notholt, J.; et al. Preliminary validation of column-averaged volume mixing ratios of carbon dioxide and methane retrieved from GOSAT short-wavelength infrared spectra. *Atmos. Meas. Tech.* **2011**, *4*, 1061–1076. [CrossRef]
26. Wunch, D.; Wennberg, P.O.; Toon, G.C.; Connor, B.J.; Fisher, B.; Osterman, G.B.; Frankenberg, C.; Mandrake, L.; O'Dell, C.; Ahonen, P.; et al. A method for evaluating bias in global measurements of CO_2 total columns from space. *Atmos. Chem. Phys.* **2011**, *11*, 12317–12337. [CrossRef]
27. Inoue, M.; Morino, I.; Uchino, O.; Miyamoto, Y.; Saeki, T.; Yoshida, Y.; Yokota, T.; Sweeney, C.; Tans, P.P.; Biraud, S.C.; et al. Validation of XCH_4 derived from SWIR spectra of GOSAT TANSO-FTS with aircraft measurement data. *Atmos. Meas. Tech.* **2014**, *7*, 2987–3005. [CrossRef]
28. Iwasaki, C.; Imasu, R.; Bril, A.; Yokota, T.; Yoshida, Y.; Morino, I.; Oshchepkov, S.; Rokotyan, N.; Zakharov, V.; Gribanov, K. Validation of GOSAT SWIR XCO_2 and XCH_4 Retrieved by PPDF-S Method and Comparison with Full Physics Method. *SOLA* **2017**, *13*, 168–173. [CrossRef]
29. Yoshida, Y.; Kikuchi, N.; Morino, I.; Uchino, O.; Oshchepkov, S.; Bril, A.; Saeki, T.; Schutgens, N.; Toon, G.C.; Wunch, D.; et al. Improvement of the retrieval algorithm for GOSAT SWIR XCO_2 and XCH_4 and their validation using TCCON data. *Atmos. Meas. Tech.* **2013**, *6*, 1533–1547. [CrossRef]
30. Ohyama, H.; Kawakami, S.; Tanaka, T.; Morino, I.; Uchino, O.; Inoue, M.; Sakai, T.; Nagai, T.; Yamazaki, A.; Uchiyama, A.; et al. Observations of XCO_2 and XCH_4 with ground-based high-resolution FTS at Saga, Japan, and comparisons with GOSAT products. *Atmos. Meas. Tech.* **2015**, *8*, 5263–5276. [CrossRef]
31. Dupuy, E.; Morino, I.; Deutscher, N.M.; Yoshida, Y.; Uchino, O.; Connor, B.J.; DeMazière, M.; Griffith, D.W.T.; Hase, F.; Heikkinen, P.; et al. Comparison of XH_2O retrieved from GOSAT short-wavelength infrared spectra with observations from the TCCON network. *Remote Sens.* **2016**, *8*, 414. [CrossRef]
32. Trent, T.; Boesch, H.; Somkuti, P.; Scott, N.A. Observing Water Vapour in the Planetary Boundary Layer from the Short-Wave Infrared. *Remote Sens.* **2018**, *10*, 1469. [CrossRef]
33. The GOSAT Data Archive Service. Available online: http://data2.gosat.nies.go.jp/ (accessed on 29 January 2019).
34. Suto, H.; Yoshida, J.; Desbiens, R.; Kawashima, T.; Kuze, A. Characterization and correction of spectral distortions induced by microvi-brations onboard the GOSAT Fourier transform spectrometer. *Appl. Opt.* **2013**. [CrossRef] [PubMed]
35. Velazco, V.A.; Deutscher, N.M.; Morino, I.; Uchino, O.; Bukosa, B.; Ajiro, M.; Kamei, A.; Jones, N.B.; Paton-Walsh, C.; Griffith, D.W.T. Satellite and Ground-based Measurements of X_{CO2} in a Remote Semi-Arid Region of Australia. *Earth Syst. Sci. Data Discuss.* **2019**. [CrossRef]
36. The TCCON Data Archive. Available online: http://tccondata.org/ (accessed on 29 January 2019).
37. Kivi, R.; Heikkinen, P.; Kyrö, E. *TCCON Data from Sodankylä, Finland, Release GGG2014R0*; TCCON Data Archive, Hosted by CaltechDATA; California Institute of Technology: Pasadena, CA, USA, 2017. [CrossRef]

38. Deutscher, N.; Notholt, J.; Messerschmidt, J.; Weinzierl, C.; Warneke, T.; Petri, C.; Grupe, P.; Katrynski, K. *TCCON Data from Bialystok, Poland, Release GGG2014R0*; TCCON Data Archive, Hosted by CaltechDATA; California Institute of Technology: Pasadena, CA, USA, 2017. [CrossRef]
39. Notholt, J.; Petri, C.; Warneke, T.; Deutscher, N.; Buschmann, M.; Weinzierl, C.; Macatangay, R.; Grupe, P. *TCCON Data from Bremen, Germany, Release GGG2014R0*; TCCON Data Archive, Hosted by CaltechDATA; California Institute of Technology: Pasadena, CA, USA, 2017. [CrossRef]
40. Hase, F.; Blumenstock, T.; Dohe, S.; Groß, J.; Kiel, M. *TCCON Data from Karlsruhe, Germany, Release GGG2014R0*; TCCON Data Archive, Hosted by CaltechDATA; California Institute of Technology: Pasadena, CA, USA, 2017. [CrossRef]
41. Warneke, T.; Messerschmidt, J.; Notholt, J.; Weinzierl, C.; Deutscher, N.; Petri, C.; Grupe, P.; Vuillemin, C.; Truong, F.; Schmidt, M.; et al. *TCCON Data from Orléans, France, Release GGG2014R0*; TCCON Data Archive, Hosted by CaltechDATA; California Institute of Technology: Pasadena, CA, USA, 2017. [CrossRef]
42. Sussmann, R.; Rettinger, M. *TCCON Data from Garmisch, Germany, Release GGG2014R0*; TCCON Data Archive, Hosted by CaltechDATA; California Institute of Technology: Pasadena, CA, USA, 2017. [CrossRef]
43. Wennberg, P.O.; Roehl, C.; Wunch, D.; Toon, G.C.; Blavier, J.-F.; Washenfelder, R.; Keppel-Aleks, G.; Allen, N.; Ayers, J. *TCCON Data from Park Falls, Wisconsin, USA, Release GGG2014R0*; TCCON Data Archive, Hosted by CaltechDATA; California Institute of Technology: Pasadena, CA, USA, 2017. [CrossRef]
44. Morino, I.; Yokozeki, N.; Matzuzaki, T.; Shishime, A. *TCCON Data from Rikubetsu, Hokkaido, Japan, Release GGG2014R2*; TCCON Data Archive, Hosted by CaltechDATA; California Institute of Technology: Pasadena, CA, USA, 2017. [CrossRef]
45. Dubey, M.; Lindenmaier, R.; Henderson, B.; Green, D.; Allen, N.; Roehl, C.; Blavier, J.-F.; Butterfield, Z.; Love, S.; Hamelmann, J.; et al. *TCCON Data from Four Corners, NM, USA, Release GGG2014R0*; TCCON Data Archive, Hosted by CaltechDATA; California Institute of Technology: Pasadena, CA, USA, 2017. [CrossRef]
46. Wennberg, P.O.; Wunch, D.; Roehl, C.; Blavier, J.-F.; Toon, G.C.; Allen, N.; Dowell, P.; Teske, K.; Martin, C.; Martin, J. *TCCON Data from Lamont, Oklahoma, USA, Release GGG2014R0*; TCCON Data Archive, Hosted by CaltechDATA; California Institute of Technology: Pasadena, CA, USA, 2017. [CrossRef]
47. Morino, I.; Matsuzaki, T.; Ikegami, H.; Shishime, A. *TCCON Data from Tsukuba, Ibaraki, Japan, 125HR, Release GGG2014R0*; TCCON Data Archive, Hosted by CaltechDATA; California Institute of Technology: Pasadena, CA, USA, 2017. [CrossRef]
48. Iraci, L.; Podolske, J.; Hillyard, P.; Roehl, C.; Wennberg, P.O.; Blavier, J.-F.; Landeros, J.; Allen, N.; Wunch, D.; Zavaleta, J.; et al. *TCCON Data from Armstrong Flight Research Center, Edwards, CA, USA, Release GGG2014R1*; TCCON Data Archive, Hosted by CaltechDATA; California Institute of Technology: Pasadena, CA, USA, 2017. [CrossRef]
49. Wennberg, P.O.; Roehl, C.; Blavier, J.-F.; Wunch, D.; Landeros, J.; Allen, N. *TCCON Data from Jet Propulsion Laboratory, Pasadena, California, USA, Release GGG2014R0*; TCCON Data Archive, Hosted by CaltechDATA; California Institute of Technology: Pasadena, CA, USA, 2017. [CrossRef]
50. Wennberg, P.O.; Wunch, D.; Roehl, C.; Blavier, J.-F.; Toon, G.C.; Allen, N. *TCCON Data from California Institute of Technology, Pasadena, California, USA, Release GGG2014R1*; TCCON Data Archive, Hosted by CaltechDATA; California Institute of Technology: Pasadena, CA, USA, 2017. [CrossRef]
51. Kawakami, S.; Ohyama, H.; Arai, K.; Okumura, H.; Taura, C.; Fukamachi, T.; Sakashita, M. *TCCON Data from Saga, Japan, Release GGG2014R0*; TCCON Data Archive, Hosted by CaltechDATA; California Institute of Technology: Pasadena, CA, USA, 2017. [CrossRef]
52. Griffith, D.W.T.; Deutscher, N.; Velazco, V.A.; Wennberg, P.O.; Yavin, Y.; Keppel Aleks, G.; Washenfelder, R.; Toon, G.C.; Blavier, J.-F.; Murphy, C.; et al. *TCCON Data from Darwin, Australia, Release GGG2014R0*; TCCON Data Archive, Hosted by CaltechDATA; California Institute of Technology: Pasadena, CA, USA, 2017. [CrossRef]
53. Griffith, D.W.T.; Velazco, V.A.; Deutscher, N.; Murphy, C.; Jones, N.; Wilson, S.; Macatangay, R.; Kettlewell, G.; Buchholz, R.R.; Riggenbach, M. *TCCON Data from Wollongong, Australia, Release GGG2014R0*; TCCON Data Archive, Hosted by CaltechDATA; California Institute of Technology: Pasadena, CA, USA, 2017. [CrossRef]
54. Sherlock, V.; Connor, B.; Robinson, J.; Shiona, H.; Smale, D.; Pollard, D. *TCCON Data from Lauder, NewZealand, 120HR, ReleaseGGG2014R0*; TCCON Data Archive, Hosted by CaltechDATA; California Institute of Technology: Pasadena, CA, USA, 2017. [CrossRef]

55. Sherlock, V.; Connor, B.; Robinson, J.; Shiona, H.; Smale, D.; Pollard, D. *TCCON Data from Lauder, NewZealand, 125HR, Release GGG2014R0*; TCCON Data Archive, Hosted by CaltechDATA; California Institute of Technology: Pasadena, CA, USA, 2017. [CrossRef]
56. The National Centers for Environmental Prediction reanalysis data. Available online: https://www.ncdc.noaa.gov/data-access/model-data/model-datasets/reanalysis-1-reanalysis-2 (accessed on 29 January 2019).
57. Nguyen, H.; Osterman, G.; Wunch, D.; O'Dell, C.; Mandrake, L.; Wennberg, P.; Fisher, B.; Castano, R. A method for colocating satellite XCO_2 data to ground-based data and its application to ACOS-GOSAT and TCCON. *Atmos. Meas. Tech.* **2014**, *7*, 2631–2644. [CrossRef]
58. Verhoelst, T.; Granville, J.; Hendrick, F.; Köhler, U.; Lerot, C.; Pommereau, J.-P.; Redondas, A.; Van Roozendael, M.; Lambert, J.-C. Metrology of ground-based satellite validation: CO-location mismatch and smoothing issues of total ozone comparisons. *Atmos. Meas. Tech.* **2015**, *8*, 5039–5062. [CrossRef]
59. Inoue, M.; Morino, I.; Uchino, O.; Nakatsuru, T.; Yoshida, Y.; Yokota, T.; Wunch, D.; Wennberg, P.O.; Roehl, C.M.; Griffith, D.W.T.; et al. Bias corrections of GOSAT SWIR XCO_2 and XCH_4 with TCCON data and their evaluation using aircraft measurement data. *Atmos. Meas. Tech.* **2016**, *9*, 3491–3512. [CrossRef]
60. Durre, I.; Vose, R.S.; Wertz, D.B. Overview of the integrated global radiosonde archive. *J. Clim.* **2006**, *19*, 53–68. [CrossRef]